THE RANDOM WALKER

Stochastic Mechano-Chemical Models for Motor Proteins

Masters Thesis

Arjun Krishnan
Adviser: Prof. Bogdan Epureanu
Department of Mechanical Engineering
University of Michigan

August 2008

Contents

List of Figures

Acknowledgements

I'd first and foremost like to thank Prof. Bogdan Epureanu, my adviser, for being extremely supportive and helpful on both professional and personal fronts. Prof. Xiuli Chao in the IOE department pointed me in the direction of renewal theory, which forms a major part of this thesis - for this I'm extremely grateful. Profs. Del Vecchio and Lafortune of the EECS department led me towards a rewarding and invaluable sidetrack studying Hybrid Systems and their relation the systems studied in this thesis.

I've had invaluable help from my peers in the Vibrations and Acoustics Lab and elsewhere. Special thanks to Adam Hendricks and Harish Narayanan.

I'd also like to thank Ms. Simmi Isaac from the ASO who has been very supportive and a great friend. I'd also like to thank my roommates Shaurjo Biswas and Harshit Sarin for entertaining exchanges of ideas, and especially for putting up with my weird hours of wakefulness and eating their food for free.

Chapter 1

Introduction

The human cell contains many mechanisms to transport nutrients, proteins and organelles. Smaller molecules like glucose can diffuse to their target locations through the cytosol - the liquid inside the cell - but larger molecules and organelles like mitochondria need to be carried from one location to another. This is done by molecular motors (also referred to as motor proteins) like kinesin, myosin and dynein, which move along track-like structures called microtubules (MTs) in the cell. One end of each molecular motor is tethered to the cargo and the other is attached to the microtubule through one or more "heads". MTs have equally spaced grooves - chemical binding sites - in which the motors heads can bind. The motor consumes adenosine triphosphate (ATP) and uses the resulting chemical energy to walk along the microtubule by moving its heads alternately from one binding site to another. Hence, kinesin is also said to "walk" hand-over-hand along the microtubule (where its heads are really legs) taking alternate steps of 8 nm each. This mechano-chemical cycle has a discrete phase of waiting and a phase of continuous motion which lead to sequential steps along MT. Single-molecule motility assays on kinesin since it's discovery nearly 25 years ago helped establish the field of single-molecule biophysics.

1.1   Motivation

Kinesin's size is of order of nanometers, and being so small is considerably affected by the collisions with the fluid molecules in its operating environment. To put the order of magnitude of these fluctuations in perspective, consider the fact that kinesin consumes about 10-100 molecules of ATP per second (Astumian 2002 [1]). ATP releases about 30 kJ of useful energy - the reaction's Gibb's free energy - per hydrolysis and this corresponds to an input power of about $3010^6/(6.023 \cdot 10^{23}) \approx 10^{-16}$ W. On the other hand, the order of magnitude of thermal energy is $k_B T$, and the relaxation time of the collisions is about 10^{-13} secs, which gives a thermal power of 10^{-8} W. Thus, the thermal fluctuations are nearly 10 times larger than the energy available to "drive" the motion. Yet kinesin manages walk for lengths of the order of micrometers and the average length of kinesin's walk is generally called it's *processivity*. The generally accepted explanation for this is that kinesin uses the energy available from ATP to *rectify* - via conformational changes, it is generally believed - these thermal fluctuations and drive itself unidirectionally, much like Feynman's thermal ratchet. The first models for molecular motors were such ratchet based models.

Molecular motors and MTs perform specialized functions in cells, and display remarkable organized, cooperative behavior. For example, many cells carry whip-like appendages like cilia or flagella (Dillon 2000 [12]) whose inner core consists of a cytoskeletal structure called the axoneme. The building block of the axoneme is the MT and each axoneme consists of several MTs aligned in parallel. Several dynein motor proteins walk synchronously on the MTs and rock them back and forth alternately to produce the flagellar "beating". The cross section of an axoneme is shown in Fig. 1.1(a).

In vivo and *in vitro* experiments (Nedelec 1997 [24]) show very interesting macroscopic organization of MTs in the presence of motor proteins. Figure 1.1(b) shows experiments and simulations in which a solution of MTs and motor proteins in a lab slide self-organize themselves into patterns (asters, vortices, etc.). What is more interesting is that the system shows phase changes; i.e., in certain regimes of MT and motor protein concentrations, certain specific types of patterns are formed.

(a) Axoneme   (b) Self-Organization and Pattern Formation
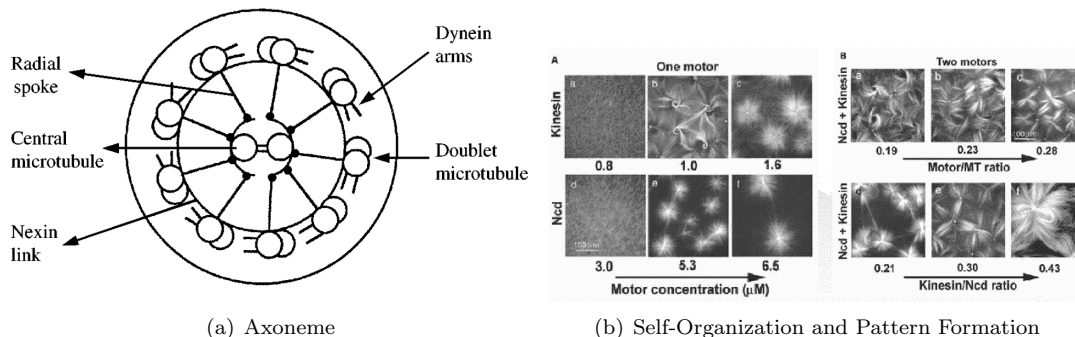
Figure 1.1: Examples of cooperative Motor Protein and MT behavior

From a mathematical perspective, kinesin is a *discrete*, *stochastic* oscillator (see Fig. 1.2). It's dynamics are hybrid, i.e., it has discrete and continuous parts, making it difficult to study using standard tools. Creating a novel description of the emergent, cooperative phenomena in a such a random environment is a considerable challenge, and this is what motivates our study. We will attempt to construct a physically consistent (parametric, as opposed to non-parametric) coarse-grained model (as opposed to an expensive molecular dynamics simulation) of kinesin using mostly known, experimentally determined parts of its mechano-chemical cycle. It is expected that such a model will give us greater insight into the physics of such nanoscale phenomena, and in the future, give us a place to start when attempting to understand similar systems.

The most interesting aspect of this problem is cooperativity. Cooperativity, coupling and synchronization between oscillators with continuous phase-space is an age old problem and has been studied extensively. There seems to be a nearly infinite range of such problems in biology, each with it's own unique quirks. Examples include the seminal work of Winfree on synchronization between "relaxation oscillators" (Winfree 1967 [38]), Mirollo and Strogatz's work on integrate and fire models for firefly sychronization (Mirollo 1990 [22]), Lacker and Peskin's work on ova maturation (Lacker 1981 [21]), Kuramoto's work on coupled oscillator lattices (Strogatz 2000 [33]); the list is endless. However, there has been very little attention given to coupling between enzymatic oscillators like kinesin; i.e., those with discrete state space, other continuous variables of interest *and* with stochastic jumps between the states. There have been recent attention given to this field of *stochastic hybrid systems* by control-theorists (Hespanha 2005 [18], Hu 2000 [19]); we choose, however, to proceed from basic stochastic processes theory to develop and extend the mathematical tools required to describe such systems and apply them specifically to the problem of motor proteins.

1.2 Experiments and Kinesin's Operating Mechanism

There are mainly two types of experiments done on kinesin. One type attempts to determine the many aspects of kinesin's chemistry and structure; these are mostly spectroscopic, kinetic and crystallographic studies and present mainly a static picture. Many key questions remain unanswered, but a general consensus regarding mechanism and structure has emerged. The other kind of experiment is the motility assay, where dynamic measurements of kinesin's processivity are made. The results of these experiments
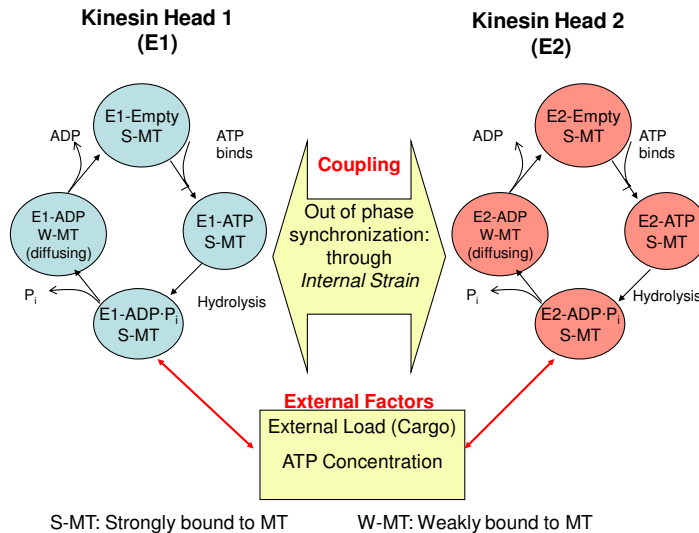
Figure 1.2: Discrete Stochastic Oscillator: schematic representation of two coupled enzymes $E1$ and $E2$ cycling through a series of states. S-MT and W-MT represent strong and weak binding to the MT.

are described in further detail below.

1.2.1 Kinesin's Structure and Chemistry

The kinesin motor protein consists of two globular domains referred or "heads". These heads are joined together by a long coiled-coiled α-helix structure called the tether or cargo-linker, which attaches to the cargo the motor transports.

The microtubule is a polymer of α and β tubulin dimers - tubulins are one of several members of a small family of globular proteins. These tubulin dimers polymerize to form protofilaments, which bundle together to form the cylindrical, hollow structure of the MT. The most important features of the MT that contribute to motor function are their *polarity* and the *chemical binding-sites* for the kinesin head on the MT spaced approximately 8 nm apart. The polarity of the MT results from the asymmetry of the monomer unit which gives each protofilament a plus-end and minus-end. This polarity determines the direction in which a particular motor protein walks. Each of kinesin's has a special region which interacts strongly with MT binding-sites and another little enzymatic pocket where nucleotides bind and hydrolyze. The MT binding region allosterically regulares the activity of the nucleobinding pocket; i.e., kinesin hydrolyses ATP much faster when bound to a MT. The heads are approximately 10 nm in diameter, and they attach and detach alternately from the binding sites on the MT to march forward. Note that since the heads are so small, they must be significantly affected by thermal fluctuations as they diffuse from one binding site to the other.

Connecting each head to the tether is a small sequence of amino acid residues called the *neck-linker*. When nucleotides bind to the head, the neck-linker undergoes a conformational change. This change is thought to produce the "power-stroke" in kinesin's cycle, throwing the trailing head forward towards the next binding site on the MT (Rice 1999 [29]). Once thrown forward, the head is close to the forward binding site, but it is not quite there. This is why it is believed that diffusion plays such an important role - the head now diffuses about in the medium until it is close enough to the next binding site and gets pulled in because of their mutual affinity.

Kinesin's chemistry is it's most extensively studied aspect, since reactions can be probed by more

tractional methods. The peculiar difficulty here is that kinesin is a *single* molecule. Each intermediate step in it's chemical cycle is also closely associated with a particular part of the mechanical cycle. Indeed, the coordination between the chemical cycles is believed to occur through internal mechanical strain. These difficulties have been overcome by particularly elegant fluorescence and mutant studies that have revealed several important aspects of kinesin's function (Guydosh 2006 [16], Rosenfeld 2003 [30]). Good estimates for the reaction rates of each chemical step (Cross 2004 [10]) have also been found experimentally. Each head of kinesin is an ATPase and is competent to hydrolyze ATP on it's own. When two heads are strongly coupled together in the kinesin dimer, their enzymatic cycles operate in synchrony and out-of-phase.

Several structures have been found that may help communicate the identity of the nucleotide bound to each head to different parts of the molecule. It is also found that the binding affinity of the head for the binding-site is strongly affected by which particular nucleotide is bound to it (Uemura 2002 [35]), and plays an important role in maintaining synchrony between the enzymatic cycles and ensuring processivity. So, we must track the chemical steps along with the associated binding affinity for the head. Let the $E \cdot (nucleotide)$ represent the enzymatic state of a kinesin head. Let S represent strong affinity for the microtubule and W represent weak affinity, where the head is free to diffuse in the medium. A typical reaction cycle for a single kinesin head can be expressed as:

$$
\begin{array}{llll}
E \cdot empty(S) & & & \text{starting state} \\
E \cdot empty(S) + ATP & \rightleftharpoons & E \cdot ATP(S) & \text{ATP binding} \\
E \cdot ATP(S) & \rightarrow & E \cdot ADP \cdot P_i(S) & \text{hydrolysis} \\
E \cdot ADP \cdot P_i \quad (S) & \rightarrow & E \cdot ADP + P_i(W) & P_i \text{ release} \\
E \cdot ADP \quad (W) & \rightarrow & E \cdot empty(S) + ADP & \text{ADP release}
\end{array}
\tag{1.1}
$$
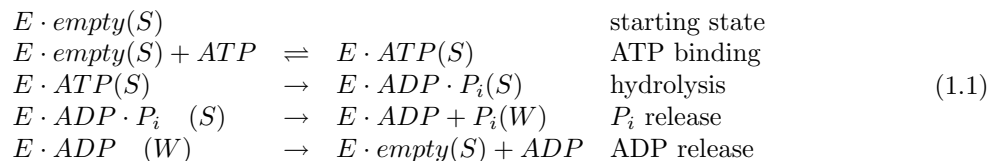
Putting all the findings from the experiments together, a generally accepted description of the mechanism is as follows (see also Fig. 1.3:

1. The starting state is one in which kinesin has just finished taking a step. The leading head is bound to the MT strongly. The trailing head has just finished hydrolysing ATP and so has ADP bound to it. This head is weakly bound to the MT.

2. ATP binds to the leading head, and produces a conformational change in the molecule that pulls the trailing head forward and closer to the next forward binding side. This is a rapid step that takes place nearly instantaneously.

3. Then, while the bound ATP molecule is being hydrolyzed by one kinesin head, the other begins a biased diffusional search for the next binding site. While this is happening, the other head is hydrolyzing it's ATP molecule.

4. When the binding site is found, the former trailing head binds strongly to it. Now, ATP binding to the (now new) leading head is prevented by the gating mechanism. When the hydrolysis is complete, P_i is released and ADP remains in the binding site. The old trailing head is now the new leading head and the motor is back to the original enzymatic state. During this cycle, kinesin has in which it has consumed exactly one molecule of ATP and advanced it's cargo by 8 nm (the head has diffused 16 nm).

The directionality of kinesin is fixed by the biased diffusional search, and a "gating" mechanism that is most-likely mediated by internal strain (Block 2007 [6]) that ensures that each step in the chemical cycle occurs sequentially in the correct order. The gating mechanism ensures that the diffusing head regains its affinity for the MT (or equivalently in terms of modelling, prevents ATP from binding to the new leading head) only *after* the trailing head finishes hydrolyzing it's ATP molecule and releases ADP. If this gating is not present, there is the possibility that ADP will be bound to both heads, reducing both their affinities for the microtubule, thereby accelerating complete detachmentment of the motor from the MT.

8
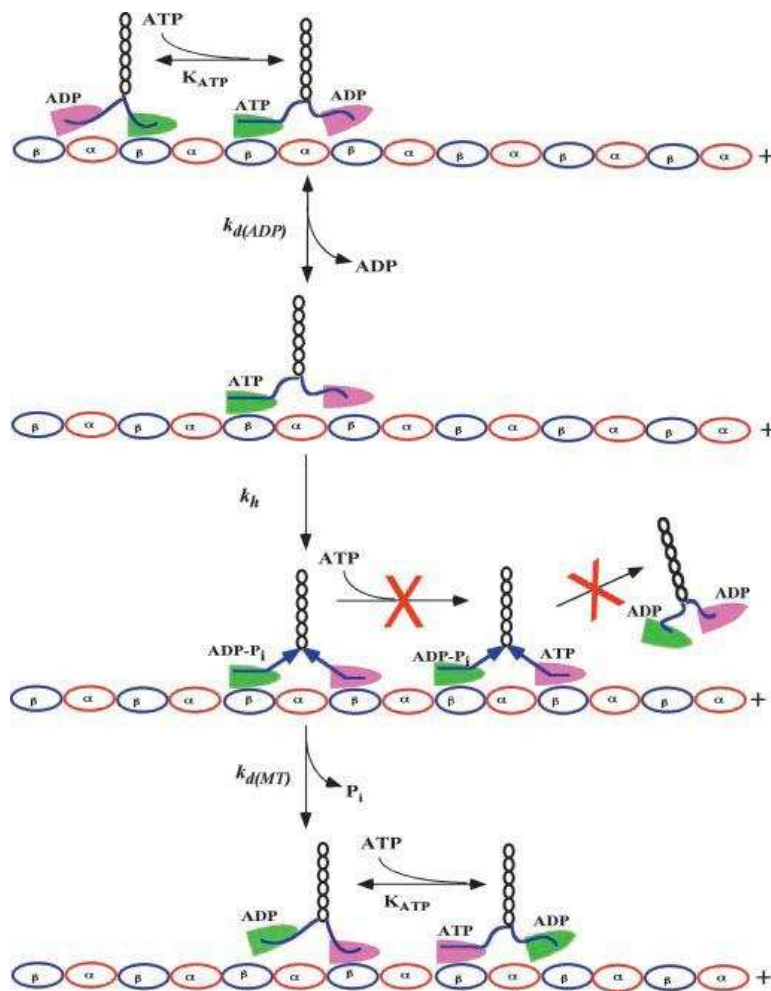
Figure 1.3: A generally accepted mechanism for the chemical and mechanical steps [30]

1.2.2 Motility Assays

Optical trap experiments are used to obtain a dynamical picture of each individual motor protein. A latex or silica bead about 1 μm in diameter is attached to the protein as it operates. The optical trap is an arrangement of lasers that can be used to exert a force on the bead (Svoboda 1993 [34]). There are many variants to this experiment differing on minor details, but essentially they all measure the bead position as a function of time. The experimental setup and a typical realization of bead position vs. time is shown in Fig. 1.4

Usually, the average velocity of the bead is one of the quantities used to quantify the processivity of the motor. Motility assays try to quantify the dependence of the bead velocity on the applied external load and ATP concentration. It is these motility assays that we will use to calibrate and test our model.

1.3 Objective

There are many models that make quantitative predictions about kinesin's motility. Some are purely kinetic models that do not include any description of the mechanical dynamics; some are purely stochas-

9
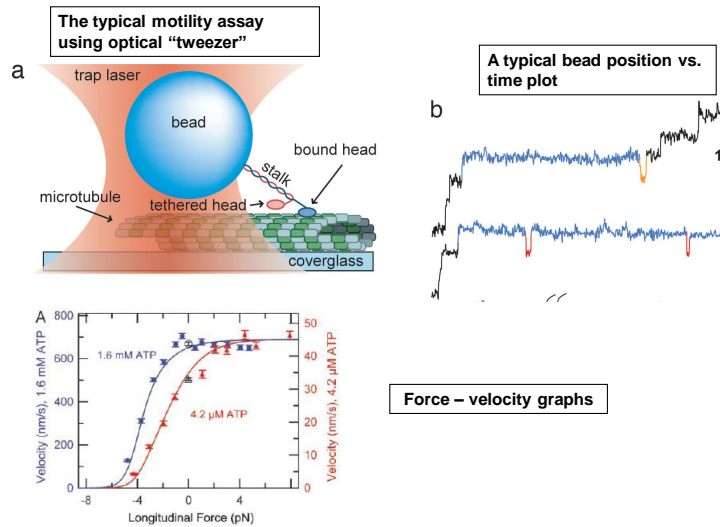
Figure 1.4: The typical setup of a motility assay and the data that is obtained from them - from [16], [5]

tic, i.e., simple Markov-chain type models that are naively fit to the data (Fisher 2001 [13]); some deal with the problem very abstractly by considering the entire motor as a single particle undergoing a Brownian motion in a fluctuating potential (Astumian 2000 [1], Reimann 2002 [28], Badoual 2002 [3], Bier 1997 [4]). The first physically consistent model that combined mechanical, kinetic and stochastic aspects of kinesin's cycle was the Peskin-Oster model (Peskin 1995 [25]). Other notable models that try to use detailed mechanics are Aztberer 2006 [2], Hendricks 2006 [17] and Derenyi 1996 [11]. Our analysis is based on the Peskin-Oster model which is henceforth referred to as the PO model. We first attempt to address the strong and weak aspects of the PO model, extend it, and develop the tools required for a more general approach. Then, we apply it to the case of two coupled motors and discuss the predictions the model makes about synchronization, velocities, randomness, etc.

Chapter 2 provides a short description of modelling the mechanics and chemistry and discusses some of the mathematics used in the later sections. Only the most essential aspects of the mathematics has been retained in the main text and involved "proofs", justifications and notes have been banished to the Appendix. Chapter 3 discusses and elaborates on different aspects of the PO model, and suggest methods of refinement and extensions. Chapter 4 discusses the application of some standard methods in the theory of stochastic processes to this particular problem, namely the concepts of first passage time and renewal theory. Chapter 5 talks about modelling the motion of multiple motors. Chapter 6 contains the summary and conclusion.

Chapter 2

Technical Introduction

This chapter has three main sections: in the first section we derive the equations of motion of the bead-kinesin system in a typical experimental setup, and quote the important results from Brownian motion theory. In the second, we describe typical chemical reaction schemes used in single molecule enzymology and their description using Markov chains. In the third, we introduce renewal theory, and quote some important results that will prove invaluable in the subsequent chapters.

2.1 Equations of Motion: The Diffusion Equations

2.1.1 Overdamped Dynamics

In a typical experiment, the two main components of the "nanotransport" system that have sufficient mass and show significant displacements to be of interest are the cargo and the kinesin heads - the enzymatic region which hydrolyzes ATP and moves from one binding site to another on the microtubule. The first approximation that comes to mind is to model these as point masses. We are only interested in their motion in the direction along the MT since this is the only coordinate measured in an experiment. The success of already existing models justifies this assumption. $3D$ models also exist which better take into account the actual structure of kinesin, but this makes the problem less susceptible to analysis and one would have to resort to Monte-Carlo simulations.

Consider the dynamics of a small particle in a fluid. Most of this material is based on Purcell's beautiful paper on swimming bacteria (Purcell 1977 [26]), with a few extensions to make our analysis more rigorous. When a very small particle moves through a fluid, its motion is characterized by its mass m, a length scale related to its size L and velocity v, and the properties of the fluid in which it is moving - density ρ and viscosity μ. When the Reynolds number of the flow around the particle is low ($Re = \rho L v / \mu \ll 1$), we can neglect the inertial terms in the Navier-Stokes equations which govern the flow, and derive what is known as Stokes' Law. Stokes' Law defines a *friction coefficient* $\gamma = 6\pi L \mu$, which can be used to include the effect of viscous fluid drag in the equations of motion of the particle as follows:

$$mx_{tt}(t) + \gamma x_t(t) = F. \tag{2.1}$$

It is important to discuss scales in this equation. First, note that when a particle is dragged in a liquid with a constant force, the solution for the velocity has the form $v(t) \sim Ae^{-t/T} + v_\infty$, where $T = m/\gamma$ is a time-constant for the exponentially decaying term, and $v_\infty = F/\gamma$ is the terminal velocity. This implies that when the force is suddenly removed, the particle comes to halt within a distance of $v_0 T$ (where v_0 is it's velocity when the force is removed) in a time T. These time and length scales are important; when they are very small, it means that inertia plays no role in the dynamics of the particle.

11

Notice that there is a "force scale" μ^2/ρ inherent in the liquid properties. Clearly, when we drag an object in a fluid with a force that is of this order of magnitude, the particle reaches a terminal velocity of $\mu^2/\rho\gamma$ and its Reynolds number is just 1. This implies that when the "dragging" force is much lower than μ^2/ρ, $Re \ll 1$.

For kinesin operating in the cell, the parameters of interest have the following values: the cytoplasm has a viscosity and density close to that of water ($\mu \approx 10^{-5} N/m^2 sec$, $\rho \approx 1000 kg/m^3$), the bead is moving with a velocity of about 500 nm/sec, has a mass of 10^{-15} kg and a radius of about 1 μm - this gives a friction coefficient of about 10^{-8} Ns/m. A kinesin head is many orders of magnitude smaller than the bead and consequently, its Reynolds number is even lower. The force-scale discussed above is 10^{-9} N for water and we deal with forces of the order of pN, which guarantees that our Reynold's number will be rather small. The important thing here is that the time constant is $T \approx 10^{-15}/(10^{-8})^2 = 10^{-7}$ sec which is small when compared to the stepping time-scales, which is of the order of ms. This means that we can just *drop* inertia in the governing equations; such motion is called *overdamped*.

The only complication here is that there is elasticity: the tether is elastic and so is the optical trap. If modelled as springs, we must include additional terms of the form $k_{sp}x$ in Eq. (2.1). The spring constant is approximately the sum of the optical trap stiffness and the tether stiffness, and that gives it an order of magnitude of 10^{-3} N/m. One obtains,

$$mx_{tt} + \gamma x_t + k_{sp}x = F(t). \tag{2.2}$$

Equation 2.2 has two eigenvalues, $\lambda = (-\gamma \pm \triangle)/2m$ where $\triangle = \sqrt{\gamma^2 - 4km}$. $\triangle$ is always less than γ when it is real. When $\triangle$ is complex, it adds oscillations to the system. We can also write the eigenvalues in terms of the more familiar non-dimensional damping ratio $-\gamma/2\sqrt{km}$ which has a value of about 10. This means that both eigenvalues are negative: one corresponds to the fast time scale and is approximately $-\gamma/m$ as before, and the other can be found by expanding the square root in a Taylor series and is $-k_{sp}/\gamma$ which is also large. Hence the dynamics continue to be overdamped.

2.1.2 The Effect of Thermal Noise: Stochastic Differential Equations

One other term we must include is a "noise", i.e., a random force $f(t)$ which is delta-correlated in time and represents the effect of thermal fluctuations. Why is noise significant here? One way of explaining this is energy argument detailed in Section 1.1. The other is the direct relation to the observed Brownian Motion of larger particles. The motor and the bead, being much smaller, must clearly also be affected. This phenomenon is well understood using Einstein's relationship and the fluctuation-dissipation theorem of statistical mechanics. Then, we may write:

$$\gamma\frac{dx_i}{dt} = \frac{\partial V(X)}{\partial x_i} + f_i(t), \tag{2.3}$$

where X is a vector containing the coordinates of interest $\{x_i\}$, $V(X)$ is the system potential energy and $f_i(t)$ is a random force on each particle i. Because of the presence of the noise, we no longer speak of a deterministic position, but a probability density function $p(x)$ of the position random variable X. Such equations are known as Langevin equations and are most efficiently handled using the tools of Stochastic Diffusion Processes. ODEs like Eq. (2.3) above are usually cast in the Ito form of the Stochastic Differential Equation (Cox 1977 [9]). Let $X(t)$ represent the position of the particle. Then we can write an equation for the increment $dX(t)$ as:

$$\gamma dX(t) = -V'(x)dt + \sigma Z(t)\sqrt{dt}, \tag{2.4}$$

where $Z(t)$ here is a purely random Gaussian process with zero mean and unit variance, and it is used to represent the effect of noise. The equation essentially means that the change in $X(t)$, *given* $X(t) = x$ in a small time dt is a normal variate with mean $V\prime(x)dt/\gamma$ and variance $\sigma^2/\gamma dt$. Let $p(x,t;x_0)$ be

the probability density for $X(t)$ with initial condition $X(0) = x_0$. Then, we can write the forward and backward Kolmogorov equations for the density as:

$$\frac{1}{2}\sigma^2 p(x,t;x_0)_{x,x} + (V'(x)p)_x - p_t = 0 \quad \text{,(Fokker-Planck or Forward Equation)} \tag{2.5}$$

$$\frac{1}{2}\sigma^2 p(x,t;x_0)_{x_0,x_0} - V'(x_0)p_{x_0} - p_t = 0 \quad \text{.(Backward Equation)} \tag{2.6}$$

While the above equation is written only for one spatial coordinate, $X(t)$ can also be a vector with many components. The generalization is obvious is be stated in the context of bead and head diffusion in Section 2.1.3.

2.1.3 The Ornstein-Uhlenbeck Process

Now that we have setup the basic stochastic differential equations, we must establish some relationships between the thermal energy $k_B T$, and the strength of the "noise" (σ) that appears in Eq. (2.5) - these are known standard results. It is useful to study this particular process because of its relationship to over-damped particles diffusing in elastic potentials. For example, at each state of the motor, the bead and head have some equilibrium positions; i.e., they diffuse in some potential well that is well-approximated by:

$$V(x) = \frac{1}{2}K_{spring}(x - x_0)^2 + fx. \tag{2.7}$$

The Ornstein-Uhlenbeck process was originally developed to show how the velocity of a particle in a fluid relaxes to the Maxwell-Boltzmann distribution (Uhlenbeck 1930 [36]). It also solves the problem of non-differentiability of sample path's in Wiener's original Brownian motion. The equation is just Newton's law in terms of the velocity U with an extra random force term, which can be expressed as:

$$dU(t) = -\beta U(t)dt + \sigma Z(t)\sqrt{dt}, \tag{2.8}$$

where β is just γ/m. Then, we can solve the Fokker-Planck equation Eq. (2.5) and obtain the probability density of the velocity $p(u,t;u_0)$ as a function of time, given an initial velocity u_0. One way to solve the equation is to take the bilateral Laplace transform of the density and solve for the moment generating function ($\phi(\theta,t) = \int_{-\infty}^{\infty} e^{-u\theta}p(u,t;u_0)du$) or cumulant generating function $K(\theta,t) = \log(\phi(t))$. It turns out that $U(t)$ is normally distributed with mean and variance:

$$E[U(t)] = u_0 e^{-\beta t}, \tag{2.9}$$

$$Var[U(t)] = \frac{\sigma^2(1 - e^{-2\beta t})}{2\beta}. \tag{2.10}$$

That is, the velocity relaxes to a normal distribution with zero mean and variance $\sigma^2/2\beta$ with a time scale of $1/\beta$. Comparing this with the Maxwell-Boltzmann equilibrium distribution for velocity, we can relate the intensity of the noise to the thermal energy as $\sigma/2\beta = k_B T/m$, and define a convenient quantity called the diffusion coefficient $D = k_B T/\gamma$ - this is Einstein's relationship. This allows us to write the Fokker-Planck equation in terms of purely physical variables instead of a "noise intensity".

For a quadratic potential $V(x)$ as in equation Eq. (2.7), Eq. (2.4) has the exact same form as Eq. (2.8), but with an origin shift. Then we conclude that the overdamped particle relaxes to its equilibrium position, the minimum of $V(x)$ at $x = x_0 - f/K_{spring}$, with a time constant given by γ/K_{spring} and an equilibrium variance of $k_B T/K_{spring}$. If we plug in typical values of tether stiffness and diffusion coefficient for the bead in a motility assay, we find that the bead relaxes to its mean position within a μs time-scale with a standard deviation in distance of about $0.5 \ nm$. Notice that the variance is *independent* of the particulars of the particle, but only on the steepness of the potential and the strength of the thermal fluctuations.

At any time, the only elements of our model that are diffusing together are the bead and one of the heads - this is obvious, since otherwise the motor would detach. We denote their coordinates and diffusion coefficients as x and D with the subscripts b and h denoting the bead and head respectively. Let $p(x_b, x_h)$ be the joint probability density and let $V(x_h, x_b)$ be the potential energy. The governing equation then generalizes to:

$$D_b \frac{\partial^2 p}{\partial x_b^2} + D_h \frac{\partial^2 p}{\partial x_h^2} + \frac{D_h}{k_B T} \frac{\partial}{\partial x_h} \left(\frac{\partial V}{\partial x_h} p \right) + \frac{D_b}{k_B T} \frac{\partial}{\partial x_b} \left(\frac{\partial V}{\partial x_b} p \right) - \frac{\partial p}{\partial t} = 0. \tag{2.11}$$

2.1.4 First Passage Time for Diffusion Processes

A useful concept to quantify the time required for a Brownian particle to traverse a certain distance is the First-Passage Time (Siegert 1951 [32], Cox 1977 [9]). To this end, we set "barriers" at $x = a, b$. These barriers serve to restrict the process to a finite spatial interval. We will use two different kinds of barriers: absorbing and reflecting. The reflecting barrier serves only to restrict the particle to a certain range, and the absorbing barrier gobbles up the particle when it hits it, signifying the end of the process. These so-called barriers just appear as boundary conditions for the diffusion equations. The chemical binding sites on the MT are exactly analogous to such absorbing barriers. When the kinesin head is diffusing and comes across a barrier, it binds, effectively ending its diffusion.

Let $g(t|x_0)$ be the first passage time density, defined for the random variable $T = sup\{t|x(t) < a\}$ where $X(t)$ is the stochastic process defined by Eq. (2.4). The equation for $g(t|x_0)$ is most conveniently written in terms of its Laplace transform (or characteristic function) defined as $g^*(s|x_0) = \int_0^\infty e^{-st} g(t|x_0) dt$. To obtain a governing equation for g^*, we note that the distribution of function $P(x, t; x_0; t_0)$ satisfies the backward equation (Eq. (2.5)) - by integrating over x - and notice that $X(t) \leq a \Rightarrow T > t$. In other words, $-g(t|x_0) = \partial P(a, t; x_0; t_0)/\partial t$. Then, we can Laplace transform the backward equation to obtain,

$$D \frac{d^2 g^*}{dx_0^2} - D \frac{1}{k_B T} \frac{dV(x_0)}{dx_0} \frac{dg^*}{dx_0} - sg^* = 0 \tag{2.12}$$

A problem of particular interest to us is diffusion between two absorbing barriers. Suppose there are two barriers at $x = a$, $x = b$ and $b < a$. Then it is clear that $g(t|x_0) = \delta(t) \Rightarrow g^*(s|x_0) = 1$ for $x_0 = a$ and $x_0 = b$, where $\delta(t)$ is the Dirac-delta function. If absorption occurs, it must occur at either a or b, and so we define the functions $g_-(t|x_0)$ as the probability density of being absorbed at b *before* it reaches a and a corresponding function $g_+(t|x_0)$. Clearly, the events being mutually exclusive, it follows that $g(t|x_0) = g_+(t|x_0) + g_-(t|x_0)$. Then the Laplace transforms of g_+ and g_- satisfy Eq. (2.12) with the boundary conditions,

$$g_+^*(s|a) = 1, \quad g_+^*(s|b) = 0, \tag{2.13}$$

$$g_-^*(s|a) = 0, \quad g_-^*(s|b) = 1. \tag{2.14}$$

Another quantity we are interested in is the limiting probability of being absorbed at a and not b and vice-versa. Call these probabilities $\pi_+(x_0)$ and $\pi_-(x_0)$. Then,

$$\pi_+(x_0) = \int_0^\infty g_+(t|x_0) dt = g_+^*(0, x_0). \tag{2.15}$$

Setting $s = 0$ in Eq. (2.12), we can solve for the limiting probabilities. Clearly, the solution is:

$$\pi_+(x_0) = \frac{\int_b^{x_0} exp(\frac{V(x)}{k_B T}) dx}{\int_b^a exp(\frac{V(x)}{k_B T}) dx}, \quad b < x_0 < a. \tag{2.16}$$
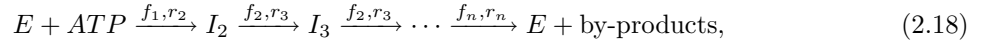
14

Clearly the solution is valid only if $V(x_0)$ is differentiable and hence well-behaved in the interval $[a, b]$. Then, $\pi_+ + \pi_- = 1$ for each x_0 if the interval is finite - we supply no proof , but it is a known fact that every point is visited infinitely often in the Ornstein-Uhlenbeck process.

A useful property of Laplace transforms for non-negative random variables such the first-passage time T, is that it serves as the moment generating function (mgf). If we want to extract the nth moment of the random variable associated with the mgf,

$$E[T^n] = (-1)^n \lim_{s \to 0} \frac{\mathrm{d}^n}{\mathrm{d}s^n} \int_0^\infty e^{-st} g(t) \mathrm{d}t = (-1)^n \lim_{s \to 0} \frac{\mathrm{d}^n g^*(s)}{\mathrm{d}s^n}. \tag{2.17}$$

2.2 Chemistry

The chemistry of a single enzyme is simply modelled using the theory of Markov processes. A typical reaction scheme for an enzyme which consumes ATP and goes through $n-1$ intermediate steps denoted by I_k, $2 \le k \le n$ is:

$$E + ATP \xrightarrow{f_1, r_2} I_2 \xrightarrow{f_2, r_3} I_3 \xrightarrow{f_2, r_3} \cdots \xrightarrow{f_n, r_n} E + \text{by-products}, \tag{2.18}$$

where f_i denotes the rate of the forward reaction from state i and r_i denotes the rate of the backward reaction from state i. Note that the intermediate states represent states of the enzyme; by-products like ADP and P_i may appear in some intermediate reaction, but their concentrations in the bulk are not going to be significantly affected by the activity of a *single* motor protein.

2.2.1 Markovian Approximation

The states of the enzyme may be considered as states of a Markov process and we may write a linear differential equation describing the evolution of the probability of each state following Qian 2002 [27]. In short, let $X(t)$ be a stochastic process taking values in E, I_k and let $\mathbf{P}(t)$ be a vector containing the probabilities of being in each state. Then we may write the forward equation for a Markov Process with discrete state space as:

$$\frac{d}{dt}\mathbf{P} = \mathbf{Q}\mathbf{P}, \tag{2.19}$$

where Q is a stochastic matrix containing the transition rates as entries. For a simple two-step reaction scheme, let $X(t)$ take values in $\{E_1, E \cdot ATP, E_2\}$ with corresponding probabilities $p_{X(t)}$. The subscripts 1 and 2 have been put in to distinguish between an initial and a final state, although they both represent the same state of the enzyme. The equation we obtain is easily solved by putting in an initial condition, and we can track the evolution of the probabilities with time.

$$E_1 + ATP \xrightarrow{k_f, k_b} E \cdot ATP \xrightarrow{kh_f, kh_b} E_2 + ADP \tag{2.20}$$
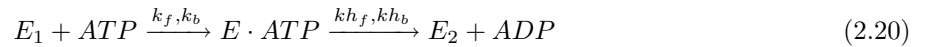
$$\mathbf{Q} = \begin{bmatrix} -k_f & k_b & 0 \\ k_f & -(k_b + kh_f) & kh_b \\ 0 & kh_f & -kh_b \end{bmatrix} \tag{2.21}$$

2.2.2 First Passage Time for the Chemistry

As in the case of diffusion processes, the first passage time of the enzyme through the reaction sequence is to be an important random variable. Consider the process defined by Eq. (2.20). Define $T = \inf\{t | X(t) = E_2, X(0) = E_1\}$. Just as we did in Section 2.1.4 for diffusion process, we make the final state absorbing

by setting $kh_b = 0$ and find that the distribution and moment generating function of T are given by,

$$\mathbb{P}\{T < t\} = F(t) = p_{E_2}(t), \tag{2.22}$$

$$E[e^{-sT}] = \int_0^\infty e^{-st} \frac{\mathrm{d}F(t)}{\mathrm{d}t} = sp_i^*(s) - p_i(0). \tag{2.23}$$

Then, after a little bookwork, it follows that $E[T] = a + b/k_f$, where a and b are some combination of the *rest* of the rate constants. In fact, we could say that this is a general form of the mean first passage time for a general reaction as in Eq. (2.18). Usually, it is justifiable to assume that the first step depends linearly on ATP concentration for a single molecule, and is the only step with any ATP dependence. Hence what this shows is that the mean first passage time for an enzyme through its enzymatic cycle from initial to final state is inversely proportional to the ATP concentration (since $k_f = k_b[ATP]$).

2.2.3 Non-Markovian Substeps

An important assumption in the above discussion on the stochastic properties assumes that the inter-arrival times of the chemical events is exponentially distributed with density ke^{-kt}; i.e., the process is Markovian in character. The most important property of such a distribution and Markov processes is it's "memorylessness". That is, the future evolution of the process from time $t = u$ given that it is at some state at that time $X(u) = A$, is independent of how the process got to A.

This assumption is good to make for the first step of ATP binding to the single-enzyme. The chance that the enzyme encounters an ATP molecule is pretty much independent of the time it has spent waiting for it; at each instant, it is equally likely that the enzyme might encounter and capture an ATP molecule. Intuitively, the *subsequent* steps like hydrolysis, however, do depend on the time at which they start. That is, the probability density function for the time of hydrolysis is no-longer exponential, but rather something more like a Gamma distribution. Assuming such a distribution for the process destroys it's Markovian character and we may no-longer write an equation like Eq. (2.20).

Nevertheless, there are ways to handle such processes, and one such way is to work with the first passage time and moment generating functions instead of dealing directly with probabilities. The other is to approximate non-Markovian densities with a series of *artificial* Markovian stages. Both are described below.

Using Moment Generating functions

To generalize the technique used in Section 2.2.1 for the first passage time to Non-Markovian inter-arrival times for chemical events, we exploit the fact that convolution corresponds to a product in Laplace space. For example, let there be two states A and B with the densities of interarrival times of the events taking the process from A to B be $f_{A,B}(t)$, $r_{B,A}$. Let $g_A(t)$, $g_B(t)$ (which we can call "hit probabilities") be the densities of the event $X(t) = A$, $X(t_-) = B$ and $X(t) = B$, $X(t_-) = A$ for $t > 0$, let $X(0) = A$ and let the superscript $*$ denote the Laplace transform of the corresponding function. Then,

$$g_A(t) = \int_0^t g_B(\tau)r_{B,A}(t-\tau)\mathrm{d}\tau, \tag{2.24}$$

$$g_B(t) = \int_0^t g_A(\tau)f_{A,B}(t-\tau)\mathrm{d}\tau + f_{A,B}(t), \tag{2.25}$$

$$\Rightarrow g_A^*(s) = g_B^*(s)r_{B,A}^*(s), \tag{2.26}$$

$$g_B^*(s) = g_A^*(s)f_{A,B}^*(s) + f_{A,}^*(s). \tag{2.27}$$

Consider a reaction sequence of the form specified in Eq. (2.18) and stochastic process $X(t)$ taking values in $\{1, 2, ..n\}$ representing the chemical state. We want the first passage time from site 1 to site n - labelled here as T. Define the "just hit state i" functions $T_i = t$ if $X(t) = i$ and $X(t^-) \neq i$, and let the

corresponding densities be $g_i(t)$ and let $f_i(t - \tau)\mathrm{d}t$ represent the probability that a transition took place from i to $i + 1$ in the time interval $(t, t + \mathrm{d}t)$, but there was no transition from $i - 1$ given $X(\tau) = i$. Define $r_i(t - \tau)$ correspondingly. Then, for $n \geq 5$ (with the cases $n = 3, 4$ being similar),

$$
\begin{align}
g_1^* &= r_2^* g_2^*, \tag{2.28} \\
g_2^* &= f_1^* g_1^* + r_3^* g_3^* + f_1^*, \tag{2.29} \\
g_k^* &= f_{k-1}^* g_{k-1}^* + r_{k+1}^* g_{k+1}^* \quad k \in \{3, ..n-2\}, \tag{2.30} \\
g_{n-1}^* &= f_2^* g_{n-2}^*. \tag{2.31}
\end{align}
$$

As before, we are looking for the function $s p_n^*(s)$ - where $p_n(t)$ represents the probability of being in state n - given by $p_n^*(s) = F_n^*(s) g_{n-1}^*$. It turns out that a general formula for the mgf of the first passage time T is of the form

$$
s p_n^*(s) = \frac{s \prod_i^{n-2} f_i^* F_{n-1}^*}{1 - \sum_1^{n-2} f_i^* r_{i+1}^* + f_1^* f_3^* r_2^* r_3^* + \cdots}. \tag{2.32}
$$

The higher order terms in the denominator can be specified in words as all products of the form $(f_{n_1}^*)(r_{n_1+1}^*)(f_{n_2}^*)(r_{n_2+1}^*) \cdots$, where the n_k are combinations of the indices where no n_k, n_j are adjacent in each term. Just as in Eq. (2.17), we can find moments of all orders using the generating function.

Method of Stages

A useful tool to approximate non-Markovian transition densities is the method of stages. It is used very often in modeling biological systems. Suppose we have a non-negative random variable T that could represent a life-time of an individual, a service time, etc. X usually has a density which has a single finite maxiumum and looks rather like a Gamma or Erlang distribution. Then, we can introduce k artificial stages, the ith stage being exponentially distributed with parameter λ_i - that is, we use a sum of exponentially distributed random variables to approximate the density. This is exactly what is being done when additional 'substeps' are introduced into a stochastic process that describes the chemical cycle of an enzyme or indeed, the mechanico-chemical cycle of a molecular motor (Fisher 2001 [13]).

There are two different ways of implementing the method of stages: one is when the stages are traversed in series, like in a chemical reaction sequence, and the other is when the stages are taken in parallel and in each realization of X the ith is chosen a probability, say π_i.

A series implementation of the method of stages amounts to approximating the Laplace transform (mgf) of the non-Markovian density as a rational function. If we expand the rational function in partial fraction form, the Laplace transform can be inverted and the density can be written as a linear combination of exponential distributions. The mgf and the corresponding density can be written as:

$$
\prod_{i=1}^{k} \frac{\lambda_i}{\lambda_i + s}, \tag{2.33}
$$

$$
\sum_{i=1}^{k} \frac{w_i \lambda_i}{\lambda_i + s}. \tag{2.34}
$$

The mean and variance of this can be fit to the observed mean and variance in an experiment, say, to determine the values of the λ_i. The mean and variance are easily found to be:

$$
E[X] = \sum_{i=1}^{k} \frac{1}{\lambda_i}, \tag{2.35}
$$

$$
Var[X] = \sum_{i=1}^{k} \frac{\sum_{i=1}^{k}(1/\lambda_i)^2}{(\sum_{i=1}^{k} 1/\lambda_i)^2}. \tag{2.36}
$$

17

2.3   Renewal Theory

A very powerful tool in the analysis of kinesin's walk is renewal theory - it's application to our problem will become clear after Chapter 3. Here, we just state some important results that we use in the next few sections. The following material is taken from the texts by Cinlar 1975 [8], Karlin 1975 [20], Ross 1983 [31] and Grimmett 2001 [15]

A renewal process $\{N(t), t \geq 0\}$ is a nonnegative, integer valued stochastic process that registers successive occurrences of an event during the time interval $(0, t]$. The time interval between events are positive, independent, identically distributed random variables, $\{X_k\}_{k=1}^{\infty}$ such that X_i is the elapsed time from the $(i-1)^{\text{th}}$ event until the occurrence of the ith event. Let the distribution of function of X_k be $F(t)$ - for us, this distribution will usually be continuous and the density will exist. Another basic stipulation is that $F(0) = 0$, meaning that $\mathbf{P}\{X_k > 0\} = 1$. Define,

$$
\begin{array}{ll}
S_n = \sum_{i=1}^{n} X_i, \ i \geq 1 & \text{Waiting Time} \\
\mathbf{P}\{S_i \leq t\} \Leftrightarrow \mathbf{P}\{N(t) \geq i\} & \text{Basic Identity} \\
E[N(t)] = M(t) & \text{The Renewal Function}
\end{array} \tag{2.37}
$$

Let μ and σ be the mean and variance of X_k. Some results we will use are as follows:

The Renewal Function The following relation is obvious from the definitions:

$$
M(t) = E[N(t)] = \sum_{j=1}^{\infty} F_j(t) \tag{2.38}
$$

Asymptotic Relationship An important result which intuition and the Strong Law of Large Numbers tells us should be true, is that the asymptotic relation $N(t) \sim t/\mu$ holds. In fact, the it holds more strongly for the mean $M(t)$ as,

$$
\lim_{t \to \infty} \frac{1}{t} M(t) = \frac{1}{\mu}. \tag{2.39}
$$

Central Limit Theorem for Renewal Processes Since the sequence $\{X_k\}_{k=1}^{\infty}$ contains identical, independently distributed random variables, a version of the central limit theorem holds. Using the fundamental identity relating S_i and $N(t)$ from Eq. (2.37), it is true that $N(t)$ is asymptotically normal with mean t/μ and variance $\sigma^2 t/\mu^3$. More precisely,

$$
\lim_{t \to \infty} \mathbf{P} \left\{ \frac{N(t) - t/\mu}{\sqrt{t\sigma^2/\mu^3}} < x \right\} = \Phi(x), \tag{2.40}
$$

where $\Phi(x)$ is the standard normal distribution.

A central result in the theory of renewal processes concerns the certain types of equations called renewal equations and their solution and long-time behavior. Many quantities of interest can be computed using this result. Although we will not use it explicitly, we state it here for the sake of completeness. An integral equation of the form (with known $a(t)$ and $F(x)$),

$$
A(t) = a(t) + \int_0^t A(t-x)dF(x) \quad t \geq 0 \tag{2.41}
$$

is called a renewal equation. Its solution is unique and is written in terms of the renewal function $M(t)$. With certain restrictions on the interarrival time distribution $F(x)$, we can comment on the long term behavior of $A(t)$ and its increments. The important relations are:

$$
A(t) = a(t) + \int_0^t a(t-x)dM(x), \tag{2.42}
$$

$$
\lim_{t \to \infty} A(t) = \frac{1}{\mu} \int_0^{\infty} a(x)\mathrm{d}x \quad \text{for } \mu < \infty. \tag{2.43}
$$

18

An important random variable connected with the renewal process is the *current life* or *age random variable* δ_t defined in terms of the waiting time S_n given in Eq. (2.37). It represents the time that has elapsed since the last renewal. We will have use for it when we use the tools of renewal theory to better understand the PO model for kinesin. The *current life* is defined as:

$$\delta_t = t - S_{N(t)}. \tag{2.44}$$

2.3.1 Renewal Reward Processes

Another variant of the renewal process that is of interest to us is the *Renewal-Reward Process*. Suppose associated with the ith lifetime is a second random variable H_i, and suppose that H_i are identically distributed and are independent. H_i is allowed to be dependent on X_i, but that the pairs $(X_1, H_1), (X_2, H_2) \cdots$ are independent. Then define the *cumulative process* $R(t)$,

$$R(t) = \sum_{k=1}^{N(t)} H_k, \tag{2.45}$$

$$\lim_{t \to \infty} \frac{E[R(t)]}{t} = \frac{E[H_k]}{E[X]}. \tag{2.46}$$

The rewards H_k need not accumulate only at the end or beginning of the renewal interval, but can increase continuously. Then, the cumulative reward is just $\tilde{R}(t) = R(t) + H_{N(t)+1}$ arising from the already elapsed part of the renewal interval. If $R(t)$ accumulates in a monotone manner, then we can use the Strong Law to get an asymptotic result. The result in terms of the expectation can also be obtained using the renewal theorem as follows:

$$R(t) \le \tilde{R}(t) \le \sum_{k=1}^{N(t)+1} H_k, \tag{2.47}$$

$$\frac{\sum_{k=1}^{N(t)} H_k}{t} = \frac{\sum_{k=1}^{N(t)} H_k}{N(t)+1} \frac{N(t)+1}{t} \xrightarrow{a.s} \frac{E[H]}{E[X]}. \tag{2.48}$$

The variance of a renewal process can be computed easily in case $N(t)$ is independent of $\{H_k\}_1^{N(t)}$. Let N be an $\mathbb{N}$ valued random variable independent of a sequence H_i of random variables and let $R = \sum_{i=1}^{k} H_i$. Let μ_N, μ_H, σ_N^2 and σ_H^2 be the variance and mean of N and H. Then, the variance of R takes the form,

$$Var[R] = \mu_H^2 \sigma_N^2 + \mu_N \sigma_H^2. \tag{2.49}$$

Many problems have a natural formulation in terms of such renewal reward processes, and one such problem is the random walk.

Chapter 3

Modelling: The Peskin-Oster Model

3.1　An Emperical Model

We begin by examining a sample path of the bead as shown in Fig. 1.4 and the head stepping pattern obtained by attaching a flouresencent tracer (Yildiz 2004 [39]). A first-approximation is to say that this resembles a Poisson counting process (or a continuous time random walk) as shown in Fig. 3.1(b)

(a) Location of the head vs. time from [39] showing kinesin steps (head location here)

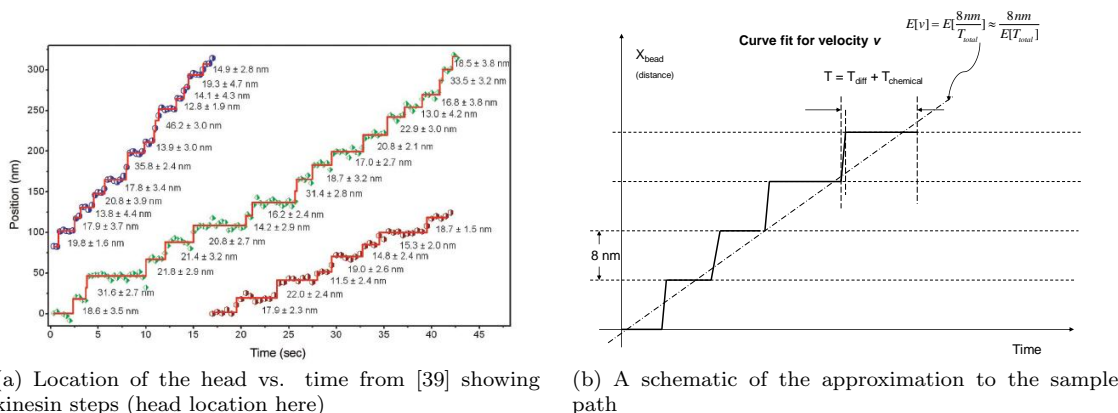(b) A schematic of the approximation to the sample path

Figure 3.1: Approximating the sample-path of the bead as steps in a poisson process

To be precise, let the bead either jumps backwards or forward at a some time T, a random variable. Note that T is distributed with density $\lambda e^{-\lambda t}$ for a Poisson stepping process. The plot of bead position vs. time suggests evidence that the bead diffusion is much faster than the chemical "dwell" times spent waiting for a reaction to complete or a nucleotide to bind.

More recent experimental work using kinesin mutants and ATP analogs(Guydosh 2006 [16]) has shown that ATP binds primarily to the leading, MT bound head, through an internal-strain "gating" mechanism. This was anticipated in Peskin and Oster's work, where they found that the ratio of the rates of ATP binding to the forward head to the backward head had to be greater than 20 to obtain good fits of the model to measured data. It is also found that backward steps are very rare and occur at the rate of one backward step to every 100 forward steps at moderate loads (Svoboda 1993 [34]).

Then it makes sense (as a first approximation) to drop the possibility of backward steps altogether. Of course, this is not really a good approximation when the forces are large. Then, diffusion limits the

rates of stepping, and backward steps become more important. Including backward steps is not too difficult, and we will discuss this in a later section. We can assume that the diffusing head binds to the forward site with probability 1, and as shown in the previous section, we can reduce the coupled diffusion processes to the diffusion of the bead alone and not worry about the head. Then the two dominant, rate limiting processes are the diffusion of the bead and the chemical reaction times, which we assume occur sequentially. For now, let us assume that the chemical processes are independent of load, and the load dependence of the velocity is brought in through the diffusion of the bead alone. However, we must state that it is believed that some form of chemical dependence on load should exist, because of the fact that the communication required for gating - lowering the rate of ATP binding of the forward head when the rear head is hydrolysing ATP - most likely occurs through the internal strain generated when stepping.

Let v be the velocity, and $E[\cdot]$, $Var[\cdot]$ represent the expectation and variance operations. The successive total cycle times, under conditions of constant load, form a sequence of independently distributed random variables. It follows from the results on renewal processes (Section 2.3) that we can write the steady-state velocity in terms of the total number completed cycles $N(t)$ as,

$$v = L \lim_{t\to\infty} \frac{N(t)}{t} = \frac{L}{E[T]} nm/sec, \tag{3.1}$$

$$T = T_{diff} + T_{chem}, \tag{3.2}$$

where $L \approx 8 \ nm$ is the distance between binding sites on a MT.

A model for the diffusion time is to use the first passage time to an absorbing barrier 8 or 16 nm away in some potential. It has been claimed in the literature that the mean first passage time grows exponentially as a function of load - clearly this depends on the potential we choose. Let us assume that the mean diffusion time is indeed exponential. The mean chemical time must be inversely related to the ATP concentration (Section 2.2.2) and so we can choose a model of the form,

$$E[T_{chemical}] = a + \frac{b}{ATP}, \tag{3.3}$$

$$E[T_{diffusion}] = c_1 e^{f c_2}. \tag{3.4}$$

The graphs in Fig. 3.2 show the model fit and a spline fit to the data. The ∘ markers are for the model curves and the □ markers are for the spline fit to the data.

The fits using this equation are shown in Fig. 3.2 and seem to capture trends rather well. However, the potential we must throw in to get the exponential dependence is ad-hoc and we must come up with a physically justifiable reason for choosing this form. What is more, since this "model" is deterministic, we have no hope of calculating stochastic properties like the randomness parameter.
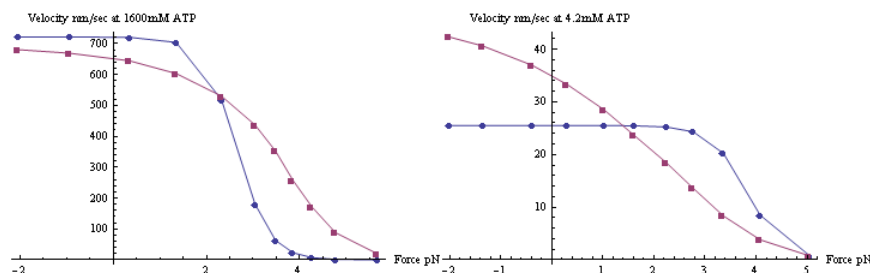

Figure 3.2: Emperical model fits to the data from [5]

21

We need to analyze the experimental setup in greater detail to come up with a better model. The discussion in the following section will show that it is not the diffusion *time* that is affected by the load, but rather it is the probability of binding forwards or backwards that is the most significant factor.

3.2 The Peskin-Oster Model

3.2.1 Model Description

The Peskin-Oster model and other variants based on it (Peskin 1995 [25], Atzberger 2006 [2], Fisher 2001 [13]) have been fairly successful in predicting various aspects of kinesin's mechanism. It is interesting to study the model to understand and justify the various assumptions that can be made. Moreover, it is essential for us to establish the theory and assumptions before we can extend it to multiple-motors.

The model is one dimensional, tracking only coordinates along the MT, and the chemistry is assumed to have only two steps, ATP binding and subsequent hydrolysis. The bead is attached to the elastic tether, which is assumed to obey Hooke's law. This is a reasonable assumption which is well-justified by the analysis in Atzberger 2006 [2], which obtains tether energies from experimental data. The other end is attached to a "hinge-point" to which both motors are attached - crystallographic studies show that the heads are attached to each other to a single point by their neck-linkers. The neck-linkers are modelled as elastic elements.

Let us define two binding states for each head as S (strongly bound to the MT) and W (weakly bound to the MT). The bead, hinge, bound head and free head locations will be called x_b, x_h, x_{bnd} and x. The hinge point is defined to be in-between the two heads at all times. The various steps in the mechanical cycle of this model can be summarized as follows:

1. The motor starts in the state $S \cdot S$. In this state, the motor is rigid and the bead undergoes a Brownian motion in some potential well established by various elastic components of the system. Then, $x_{bnd_1} = 0, x_{bnd_2} = 8, x_h = 4$.

2. Now, ATP binds to one of the two heads and the system undergoes a transition $S \cdot S \rightarrow S \cdot W$, i.e., one of the heads is now weakly bound and is free to diffuse in a potential biased towards the next forward binding site. This biasing potential is another modelling input and one simple choice is to assume it is quadratic. Suppose ATP binds to the forward head. Then, $x_{bnd} = 8 \ nm, x_h = 8 + x_0, x = 8 + 2x_0$

3. While the ATP hydrolysis is taking place, the free head and the bead diffuse together, governed by an equation of the form given by Eq. (2.11).

4. As soon as ATP hydrolysis completes, the free head regains its affinity for the MT and quickly finds a free binding site to attach to. The potential in which the head diffuses is biased in the forward direction, by defining a "power stroke". That is, the minimum of the biasing potential located close to the forward bind site.

5. Once this binding takes place, ATP hydrolysis is completed and the by-products of the hydrolysis are ejected from the nucleotide binding pocket. This brings the system back to its original state $S \cdot S$ with both heads free of nucleotide. One of the heads has travelled a distance of 16 nm and the bead has moved 8 nm, the spacing on the MT.

The model paramters are:

- β_b = ATP binding constant for the forward head or unbinding rate constant for the backward head.

- β_f = ATP binding constant for the backward head or unbinding rate constant for the forward head.

22

- α = hydrolysis rate of ATP.

- L = distance between two binding sites on the MT (8 nm).

- x_0 = "power stroke" distance, or equilibrium position of the diffusing head. This is positive and biased towards the forward binding site.

- K_{th}, K_{bias} = tether and bias potential stiffness (both quadratic).
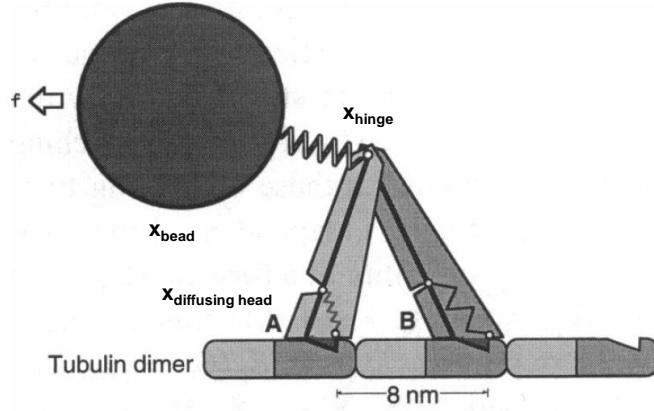

Figure 3.3: Schematic of the PO model [25]

There are just two distinct states of the motor in the model - either both heads are attached to the MT or one head is attached and the other is diffusing. The absolute position of the motor is kept track of by indexing the binding sites on the MT with integers. Peskin and Oster keep track of the position *and* chemical state of the motor simultaneously by allowing the index to take half-integer values - this is an elegant method, but can be easily dispensed with while using the tools of renewal theory. That is, when both motors are bound to the MT, the state $s = k$ is some integer. The leading head is at kL and the other is at $(k-1)L$, with the hinge in-between at $(k-1/2)L$. After ATP binds, if the rear head comes unbound, $s = k + 1/2, x_{bnd} = kL, (k-1)L \leq x \leq (k+1)L$. If the leading head is released, $s = k - 1/2, x_{bnd} = (k-1)L, (k-2)L \leq x \leq kL$. For a single motor, it will not prove essential to keep track of the index k to get steady-state behavior, but we leave it in here for use in the discussion on multiple-motors. Let $\mathbb{I}$ represent the set of integers, and let $\mathbb{H}$ be the set of half-integers. To summarize:

$$x_{bnd}(k) = \begin{cases} kL, & k \in \mathbb{I} \\ \left(k - \frac{1}{2}\right) L. & k \in \mathbb{H}. \end{cases} \tag{3.5}$$

The diffusion equations governing the motion of the bead and head must be solved in two potentials, one for each kind of state. We can write these potentials in the two states as $\phi_1(f, x_b, k)$ and $\phi_2(f, x_b, x, k)$, in terms of the bead position, state index and free head location (or equivalently, the hinge $x_h = (x_{bnd} + x)/2$), as follows:

$$\phi_1(f, x_b, x_h, k) = f(x_b - x_h) + \frac{1}{2}K_{th}(x_b - x_h)^2, \tag{3.6}$$

$$\phi_2(f, x_b, x, k) = f(x_b - x_h) + \frac{K_{th}}{2}\left(x_h - x_b\right)^2 + W(x_h - x_{bnd}), \tag{3.7}$$

where $W(x)$ denotes an interaction potential (whose form they don't specify) that biases the diffusion of the head towards forward binding-site. Following [2], we also model the interaction potential as $W(x) = 1/2K_{bias}(x - x_0))$.

23

The PDEs Eq. (2.11) for the coupled diffusion of the bead and head are difficult to solve in general, but certain observations simplify the problem considerably. The bead is about nearly a 1000 times larger than the head and since the diffusion coefficient is inversely proportional to size, we can set $D_h \to \infty$. This essentially amounts to a separation of time-scales. It implies that the head rapidly equilibriates with the bead. Then dividing Eq. (2.11) by D_h and setting it to ∞, we get:

$$\frac{\partial^2 p}{\partial x_h^2} + \frac{1}{k_B T} \frac{\partial}{\partial x_h} \left(\frac{\partial V}{\partial x_h} p \right) = 0. \tag{3.8}$$

Note that now $\rho(x|x_b)$ is a conditional probability, meaning it represents the position of the head, given bead position. The solution to this equation is the Boltzmann equilibrium density:

$$\rho(x|x_b, k) = \frac{exp\left(\frac{-\phi_2(x_b, x, k)}{k_B T} \right)}{\int_{-(k-3/2)L}^{(k+1/2)L} exp\left(\frac{-\phi_2(x_b, x, k)}{k_B T} \right) dx}. \tag{3.9}$$

Then using the identity for the joint density $p(x, x_b) = \rho(x_h|x_b)p(x_b)$ and integrating over the allowed range for x_h (between the binding sites), we can write an *effective potential* for the bead in which it diffuses with its own D_b, mathematically independent of the head location. The effective potential takes the form:

$$\phi_{eff} = -k_B T \log \left(\int_{-(k-3/2)L}^{(k+1/2)L} exp \left(\frac{-\phi_2(x_b, x, k)}{k_B T} \right) \right). \tag{3.10}$$

Once ATP hydrolysis completes, we can employ the previously mentioned separation of time-scales and do a fast-time scale analysis to find whether the head binds forwards or backwards. Peskin and Oster present a slightly different method of finding this probability using the Fokker-Planck equation, but the formula is immediate from the backward equation and the first passage time formulation (Section 2.1.4). Given some x_b, x the eventual probability of absorption at the forward binding site is given by an equation similar to Eq. (2.15). Then, to find the total probability of binding forwards $p_t(x_b, k)$, given bead position x_b can be written as,

$$\pi(x, x_b) = \frac{\int_b^x exp(\frac{\Phi(x_b, x')}{k_B T}) dx'}{\int_b^a exp(\frac{V(x')}{k_B T}) dx'}, \tag{3.11}$$

$$p_t(x_b, k) = \int_{-(k-3/2)L}^{(k+1/2)L} \pi(x, x_b) \rho(x|x_b, k) dx. \tag{3.12}$$

Peskin and Oster make the claim that the bead diffusion time is insignificant - that is, that the bead settles down into the Boltzmann density $\rho_{bead}(x_b, k)$ nearly instantaneously in the effective potential. Then, the total probability of binding forwards $P(f)$ can be written as:

$$P(f) = \int_{-\infty}^{\infty} p_t(x_b, k) \rho_{bead}(x_b, k) dx_b. \tag{3.13}$$

A Markov chain can be constructed on the stochastic process $X(t) = j$, where j is the state variable that keeps track of the motors "phase" and its location. Let $C_j(t)$ be the probability of finding the system in state j. For integer j,

$$\frac{dC_j}{dt} = \alpha P C_{j-1/2} + \alpha(1 - P)C_{j+1/2} - (\beta_b + \beta_f)C_j, \tag{3.14}$$

$$\frac{dC_{j+1/2}}{dt} = \beta_b C_j + \beta_f C_{j+1} - \alpha C_{j+1/2}. \tag{3.15}$$

The mean and variance of $X(t)$ - denoted by $M(t)$ and $V(t)$ - can be obtained from Eq. (3.14) by summing with appropriate weighting of each equation over the index j. The solution is presented here for later comparison:

$$L\frac{dM(t)}{dt} = \frac{L\alpha}{\alpha+\gamma}\left(\left(p-\frac{1}{2}\right)\gamma+\frac{\delta}{2}\right), \tag{3.16}$$

$$L^2\frac{dV(t)}{dt} = \frac{L^2\alpha\gamma}{\alpha+\gamma}\left\{1-\frac{4\left(\alpha\left(P(f)-\frac{1}{2}\right)-\frac{\delta}{2}\right)\left(\gamma\left(P(f)-\frac{1}{2}\right)-\frac{\alpha\delta}{2\gamma}\right)}{(\alpha+\gamma)^2}\right\} \tag{3.17}$$

3.2.2 Fits using the Peskin-Oster model

Since we have made some slight changes to the PO model, namely, a simpler biasing potential $W(x)$ and fits to more recent data (Block 2003 [5]) at different ATP concentrations, we compute the fits once again. The fit parameters we obtain will come in handy when we extend the model to multiple motors - i.e., we are able to make a uniform comparison between single and multiple-motor predictions. Since we only seek a qualitative comparison, the quality of the fit itself is not of prime importance in our study.

We continue to use the same parameters and procedure from [2] and [25] to fit for the higher ATP concentration. Then γ is changed, keeping the ratio of β_b/β_f constant, to obtain a fit for the lower ATP concentration. The predicted randomness parameter using these parameters are plotted against the experimental data. It is noted here that the predicted randomness for the higher ATP concentration is marginally higher than the data, indicating that there may be more steps in the chemistry.

(a) Force vs. Velocity, ATP = 1600 μM (b) Force vs. Velocity, ATP = 4.2 μM

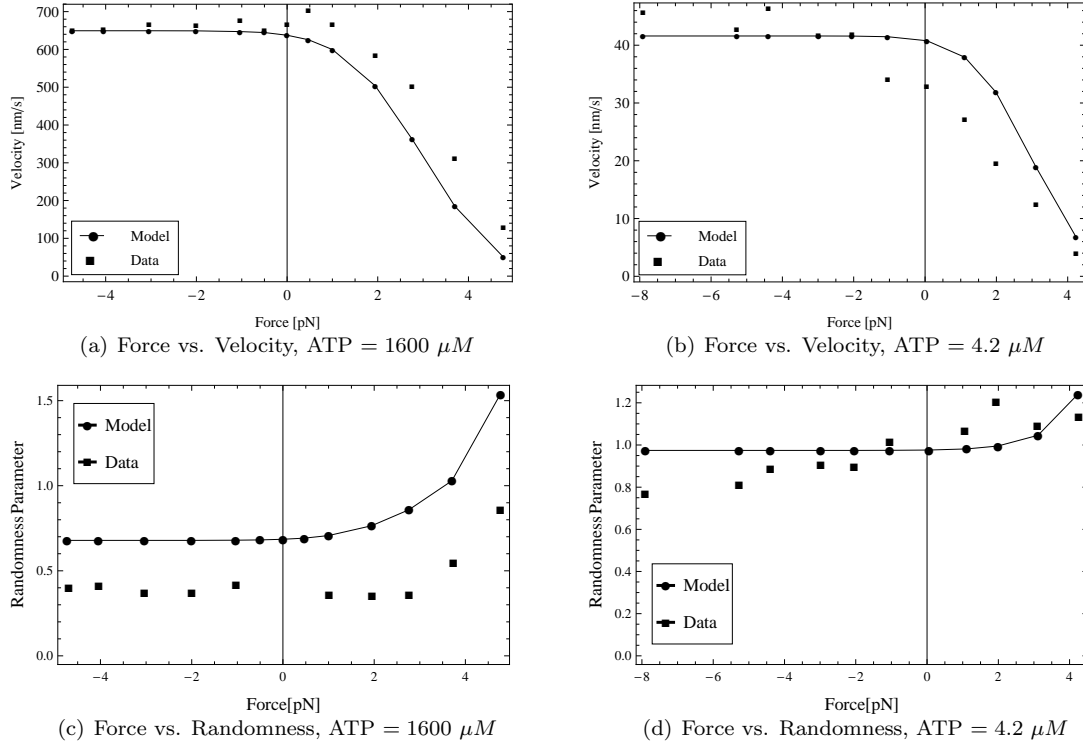(c) Force vs. Randomness, ATP = 1600 μM (d) Force vs. Randomness, ATP = 4.2 μM

Figure 3.4: Fits to the velocity and randomness parameter from [5] using the Peskin-Oster model

3.3 Some Aspects of the Peskin-Oster Model

3.3.1 The Head Conditional Density

Consider the head density given by Eq. (3.9). To calculate the probability of binding forwards or backward, Peskin and Oster restrict the head's location to within the binding sites by normalizing the density. Then the mean location $E[x|x_b] = \int_a^b x\rho(x|x_b, k)$, clearly, must lie between a and b. Variables a and b specify the finite interval of integration $((k-3/2)L, (k+1/2)L)$ and are used in the following few sections purely for notational convenience. There is a reason for restricting the head: the formula derived for the binding probability from the backward equation, Eq. (2.16) is valid only if the point from which the diffusion begins is in (a, b).

A few comments are in order here. For diffusion in some potential, $V(x_1, x_2)$, if we can separate the diffusion time-scales (or even otherwise), the joint equilibrium density $\rho(x_1, x_2)\rho(x_2)$ is given by the conditional density and the effective potential as in Eq. (3.9) and Eq. (3.10). It is clear that the joint density has maxima where $V(x_1, x_2)$ has minima - let this be at some single point $(\bar{x}_1, \bar{x}_2)$. If x_1 is artificially restricted to an interval (a, b) which is not infinite, the equilibrium position of x_1 given by the minimum of $V(x_1, x_2)$ may lie outside this interval and this will in-turn change the equilibrium location of x_2 in its effective potential. In fact, the mean locations will be different even if the $\bar{x}_1$ lies in (a, b) because of the restriction. The truncated and unrestricted densities are shown in Fig. 3.5. The new mean locations due to the restriction are also indicated.

However, the mean locations will not prove to be an issue in kinesin's walk, since the process effectively stochastically renews itself once the motor steps, and the step size is 8 nm, no matter what.
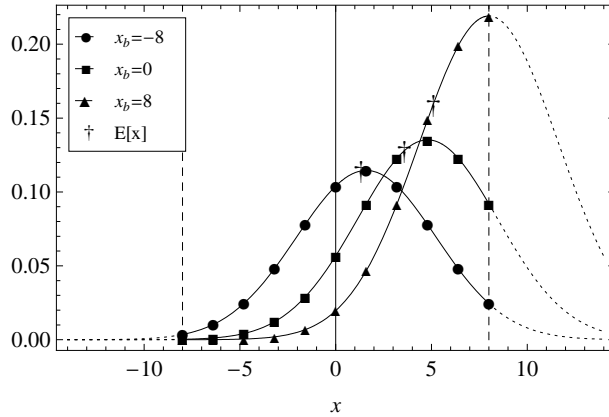

Figure 3.5: Trucation of the probability density of the head for different bead locations

Nevertheless, since the equilibrium standard deviation for our problem given by Eq. (2.9) is about $3 - 4$ nm for both the head and the bead and as long as $\bar{x}_1$ lies comfortably within the interval (a, b), the mean positions of the bead and the head will be quite close to $(\bar{x}_1, \bar{x}_2)$. It is not necessary for us to check this analytically, because it turns out that it is not a factor at all (see Section 4.1).

One way out is to not restrict the head at all, and redefine the probability of binding forwards. Note that the Ornstein Uhlenbeck process is recurrent in the sense that starting from any x_0, every point is reached eventually with probability 1 (Cox 1977 [9]). So if $x_0 > b$, it will bind to b definitely and will not if $x_0 < a$. Then,

$$p_t(x_b, k) = \begin{cases} 0 & -\infty < x < a \\ \int_{-b}^{a} \pi(x_b, x)\rho(x|x_b, k)\mathrm{d}x & a \le x \le b \\ 1 & b < x < \infty \end{cases}. \tag{3.18}$$

26

However, if we do not restrict the head, the head may bind to other binding sites *outside* the region (a, b). So, another way around this is to solve for the equilibrium density after restricting the head using appropriate boundary conditions at the end points of the region of interest, say, by using reflecting barriers.

3.3.2 The Effective Potential

One assumption made in Section 3.3.1 is that the effective potential was assumed to be quadratic (for the variance and time-scale estimates to apply). This is indeed true when the head is unrestricted as can be checked by direct integration, but when it is restricted in the fashion of Peskin and Oster, the stiffness of the effective potential does indeed change and is *no longer* quadratic. If it is significantly different from quadratic, then formulas in Section 2.1.3 do not apply. We then have no real estimate of the time-scales of diffusion and of the variance, both important to the PO model.

What we can do is estimate the deviation from quadraticity of the effective potential by finding second and higher derivatives in the Taylor expansion of the potential about the mean location (and finding bounds). Consider the system potential energy $\phi_2(x, x_b)$ defined by Eq. (3.6) and the effective potential $\phi_{eff}(x_b)$. The bead equilibrium position is where the derivative of $\phi_{eff}(x_b)$ vanishes at some $\bar{x}_b$, where

$$\frac{d\phi_{eff}(x_b)}{dx_b} = \frac{\int_a^b \frac{\partial \phi_2(x_b, x)}{\partial x_b} exp\left(\frac{-\phi_2(x_b, x)}{k_B T}\right)}{\int_a^b exp\left(\frac{-\phi_2(x_b, x)}{k_B T} dx\right)}. \tag{3.19}$$

Since the exponential is a positive, continuous function, for each fixed x_b, the mean-value theorem for integration applies to the integral in the numerator. Also note from Eq. (3.6) that for every fixed x_c, there exists an corresponding $\bar{x}_b$ such that the $\partial \phi_2(\bar{x}_b, x_c)/\partial x_b$ vanishes. Then, we obtain,

$$\frac{\int_a^b \frac{\partial \phi_2(x_b, x)}{\partial x_b} exp\left(\frac{-\phi_2(x_b, x)}{k_B T}\right)}{\int_a^b exp\left(\frac{-\phi_2(x_b, x)}{k_B T} dx\right)} = \frac{\partial \phi_2(x_b, x_c(x_b))}{\partial x_b} \quad a < x_c(x_b) < b \tag{3.20}$$

$$\bar{x}_b = -\frac{f}{K_{th}} + \frac{1}{2}\left(x_c(\bar{x}_b) + \left(k - \frac{1}{2}\right)L\right) \tag{3.21}$$

Further, note that $d^k \phi_2(x_b, x)/dx_b^k$ is K_{th} for $k = 2$ and identically zero for all higher derivatives. Using this fact we can write:

$$\frac{d^k \phi_{eff}(x_b)}{dx_b^k}\bigg|_{\bar{x}_b} = \begin{cases} K_{th} - \frac{\int_a^b \frac{1}{k_B T}\left(\frac{\partial \phi_2(x_b, x)}{\partial x_b}\right)^2 exp\left(\frac{-\phi_2(x_b, x)}{k_B T}\right)}{\int_a^b exp\left(\frac{-\phi_2(x_b, x)}{k_B T} dx\right)}, & k = 2 \\ \frac{\int_a^b \left(\frac{1}{k_B T}\right)^{k-1}\left(\frac{\partial \phi_2(x_b, x)}{\partial x_b}\right)^k exp\left(\frac{-\phi_2(x_b, x)}{k_B T}\right)}{\int_a^b exp\left(\frac{-\phi_2(x_b, x)}{k_B T} dx\right)}, & k = 3 \end{cases} \tag{3.22}$$

For each $k > 1$, there is a $x_{c_k}(x_b) \in (a, b)$ such that the mean value theorem applies to integrand in numerator of the RHS of Eq. (3.22). After a little algebraic manipulation we obtain,

$$\frac{\int_a^b \left(\frac{1}{k_B T}\frac{\partial \phi_2}{\partial x_b}\right)^k exp\left(\frac{-\phi_2(x_b, x)}{k_B T}\right)}{\int_a^b exp\left(\frac{-\phi_2(x_b, x)}{k_B T} dx\right)}\bigg|_{\bar{x}_b} = \left(\frac{\partial \phi_2}{\partial x_b}\right)^k = \left(\frac{1}{2}K_{th}(x_{c_k} - x_c)\right)^k. \tag{3.23}$$

There are more terms in higher derivatives, but the key is that they of the form $(K_{th})^m (K_{th}L)^n/(k_B T)^{n-1}$, where m, n are positive integers. Thus, all we require is that $(K_{th}L)^2/(k_B T)$ is small. We use $K_{th} = 0.25\ pN/nm$ - it's actually about $0.15\ pN/nm$ [2] - the thermal energy is around $4.14\ pN \cdot nm$ and

27

$L = 8$ nm - so we seem to be in safe territory. To gain further confidence, we plotted the effective potentials for a range of forces in Fig. 3.6 which shows that the potential remains nearly quadratic, and has a stiffness not very different from 0.25 pN/nm, thus placing a definite time-scale on the bead diffusion for all forces. This time-scale is γ/K_{th} of the order of 1 μs and thus it is reasonable to assume that the bead diffusion is nearly instantaneous compared to the chemical times.
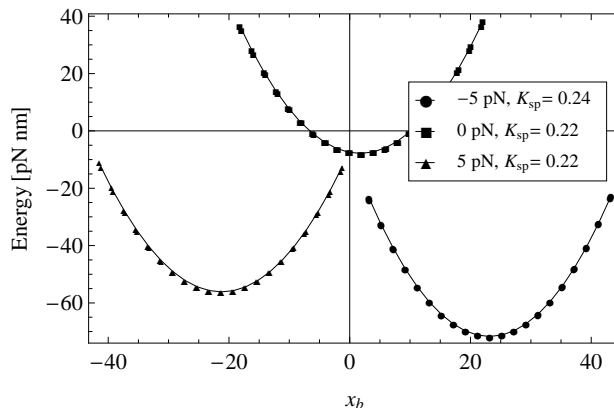

Figure 3.6: Effective potentials on the bead for different loads and quadratic fits to them

3.3.3   Substeps in the Model

One important feature of the model is that it shows substeps. We must go through the construction of the model to see why: the dynamics begin in the state when both heads are bound to the MT and the bead is at its equilibrium location. Once ATP binds, one head is freed and the bead settles into a new equilibrium position, waiting for hydrolysis to take place. The hydrolysis time used by Peskin and Oster (from Gilbert 1995 [14]) is on average about 0.0025 sec. Once hydrolysis completes, the motor steps forward (or backward) and the bead moves a total distance of 8 nm. Moreover, this substep is of variable size; its size depends on load. A plot of this substep is shown in Fig. 3.7. The figure also shows the effect of restricting the head between the binding sites on the substep size. Note that if the head is unrestricted, its mean position may not be in between the sites of interest, and substeps may also be *negative*. This is one good physical reason to restrict the head location.

In the PO model, when the bead and head are both diffusing, the bead is assumed to move by exactly half of the site-spacing - hence the indexing by half-integers in Eq. (3.14). In the light of the above paragraph this is clearly not true and there is, in fact, a load dependence for the size of the substep. However, as shown in the following chapter, this will not make a difference to the long-time mean location or even variance of the bead. To summarize, substeps exist in the PO model, but their size does not appear in the formulas for the steady-state velocity and randomness parameter.

There have been differing opinions on whether kinesin shows substeps or not. Some believe that it does, and various groups conducting different experiments have found substeps of differing lengths and duration [37], [6]. Carter and Cross (Carter 2005 [7]) however, performed rigorous analysis of the position time series obtained from the experiment and determined that there are no substeps even on the μs time scale.

Since this is just a model - and one-dimensional in any case - various aspects remain purely hypotheses. The modelling choices will become clearer as a three dimensional picture of kinesin's walk emerges from further experiments. We might be tempted to hypothesize that there might be a rotational aspect to the head's motion as it steps hand-over-hand (Yildiz 2004 [39]). The origin of the force-production in
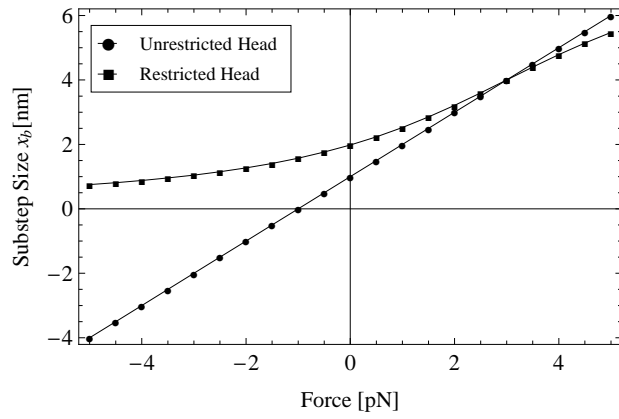
Figure 3.7: Substep size as a function of load for an unrestricted and restricted head

kinesin, it is generally believed, might be from a conformational change in the neck-linker region. This might induce a rotational strain in the coiled tether which throws the rear-head forwards.

Chapter 4

Extensions to the Peskin-Oster Model

As we have seen earlier, the PO model has some deficiencies, and our objective here is to provide some extensions based on renewal theory. One of the main focuses is to include the effects of non-Markovian chemical processes for the hydrolysis, a greater number of steps in the chemical reaction itself and a diffusion time, if needed.

4.1 Renewal Theory Formulation of the Peskin-Oster Model

Let kinesin's cycle be as described in the PO model. We now allow the hydrolysis process to be made up of k chemical steps as in Eq. (2.18), and allow the transitions densities to be non-Markovian. Suppose we need to account for the diffusion of the bead. If we can assume that it is one of the steps of the *sequential* chemical process - i.e., no processes are taking place in parallel - a good model, as stated before is the first passage time. We may summarize the steps in the model as follows:

1. We begin in the state where both heads are strongly bound to the MT. ATP binds to either the forward head or backward head with rates β_b and β_f. The arrival time for this event T_b, clearly, must be exponentially distributed with density $(\beta_b + \beta_f)\exp(-(\beta_b + \beta_f)t)$

2. Once ATP binds, the bead comes to a new equilibrium position, hydrolysis begins and this is a sequence of k chemical steps. The time required for this to take place is written as $T_h + T_{d_1}$ where the subscripts h and d_1 correspond to hydrolysis and the first bead diffusion

3. When hydrolysis completes, the head searches for the next binding site and binds forwards (backwards) with probability p $(1-p)$.

4. The bead then diffuses to its new equilibrium position in T_{d_2} and the cycle is complete.

Then consider the sequence of total times $\{T_i\}$, the renewal process constructed on it $N(t)$ with renewal function $M(t)$, variance $V(t)$, the associated reward sequence $\{H_i\}$ and cumulative reward $R(t)$ defined as:

$$T_i = T_b + T_h + T_{d_1} + T_{d_2}, \tag{4.1}$$

$$R(t) = \sum_{k=1}^{N(t)} H_k. \tag{4.2}$$

$$H_i = \begin{cases} L \\ 0 \\ -L \end{cases} \quad \text{with probability} \quad \begin{matrix} \frac{\beta_b}{\beta_b + \beta_f} p \\ \frac{\beta_b}{\beta_b + \beta_f}(1-p) + \frac{\beta_f}{\beta_b + \beta_f} p \\ \frac{\beta_f}{\beta_b + \beta_f}(1-p) \end{matrix} . \tag{4.3}$$

This defines a renewal reward process with limiting mean and variance $M_R(t), V_R(t)$ of the cumulative reward function given by Eq. (2.45) and Eq. (2.49). In the case of the Peskin-Oster model, $T_{d_i} = 0$, the hydrolysis and binding rates are exponential with rates α and $(\beta_b + \beta_f)$. As before, $\gamma = \beta_b + \beta_f$ and $\delta = \beta_b - \beta_f$ and,

$$E[T_i] = \frac{\alpha\gamma}{\alpha + \gamma} \tag{4.4}$$

$$E[H_i] = L\left(\frac{\delta}{2\gamma} + \left(p - \frac{1}{2}\right)\right) \tag{4.5}$$

$$\text{velocity} = \frac{E[H_i]}{E[T_i]} = \frac{L\alpha}{\alpha + \gamma}\left(\left(p - \frac{1}{2}\right)\gamma + \frac{\delta}{2}\right) \tag{4.6}$$

To fit the randomness parameter, we need to find the limiting variance of the reward process. This is obtained from Eq. (2.49) and simplified using the variance and mean of the renewal process from Eq. (2.3) to obtain,

$$\lim_{t\to\infty} \frac{V_R(t)}{t} = \mu_{H_i}^2 \frac{V(t)}{t} + \frac{M(t)}{t}\sigma_{H_i}^2, \tag{4.7}$$

$$\lim_{t\to\infty} \frac{V_R(t)}{t} = \frac{L^2\alpha\gamma}{\alpha + \gamma}\left\{1 - \right.$$

$$\left. \frac{4\left(\alpha\left(P(f) - \frac{1}{2}\right) - \frac{\delta}{2}\right)\left(\gamma\left(P(f) - \frac{1}{2}\right) - \frac{\alpha\delta}{2\gamma}\right)}{(\alpha + \gamma)^2}\right\}. \tag{4.8}$$

The equations for the velocity and variance are identical to the PO model in Eq. (3.16). It is interesting to note that even though we have not included the substeps in the reward function - the haf states in Eq. (3.14) - the mean and variance are still identical (but see also Eq. (2.47)). As discussed in Chapter 5, it turns out that even for two motors pulling a load, the long-time variance and mean are independent of the substep size.

If in the future we wish to investigate transient behavior of the variance or mean, where the effect of substeps should be more apparent, we must more precisely define the cumulative reward process $R(t)$. We may define $R(t)$ in terms of the renewal current life δ_t from Eq. (2.44), the time elapsed since the last renewal. That is, we must include the possibility that from the both-heads-bound state, an ATP binding event has occurred and hydrolysis has not yet been completed, throwing the motor into a half-integer state, and the bead performs a substep of size $0 < \tilde{L} < L$. Let this substep be represented by a terminal reward $\tilde{H}$, and $R(t) = \sum_{k=1}^{N(t)} H_k + \tilde{H}(t)$, where

$$\tilde{H} = \begin{cases} \tilde{L} & \text{with probability } \left(1 - e^{-(\beta_b + \beta_f)\delta_t}\right)\frac{\beta_b}{\beta_b + \beta_f} \\ -\tilde{L} & \text{with probability } \left(1 - e^{-(\beta_b + \beta_f)\delta_t}\right)\frac{\beta_f}{\beta_b + \beta_f} \end{cases} \tag{4.9}$$

4.2 First Passage Time Formulation: The Imbedded Chain

Consider a random walk in continuous time $X(t)$ taking values in the integers, with time-homogeneous probability densities of transition forwards and backwards from site i given by $\lambda_i(t)$, $\mu_i(t)$ respectively.

Suppose the initial condition for the process is $X(0) = 0$. Then define the time-increments of the renewal process as the first passage time to site 1. That is,

$$T_i = inf\{t|X(0) = 0, X(t) = 1\}' \tag{4.10}$$

Intuitively, each time the motor steps to the next site, the process 'renews' itself and is stochastically identical thereafter. How do we calculate this first passage time? As before, we make site 1 an absorbing barrier for the continuous time random walk, and define the "first-hit" densities $g_i(t)$ and their Laplace transforms $g_i^*(s)$ for each site $i < 1$ as in Section 2.2 as,

$$g_0^* = \lambda_0^* g_{-1}^* \tag{4.11}$$
$$g_k^* = \lambda_{k-1}^* g_{k-1}^* + \mu_{k+1}^* g_{k+1}^* \quad k \leq 0 \tag{4.12}$$

Again, we are looking for the mgf of the first passage time T defined as $sp_1^*(s)$ - where $p_n(t)$ represents the probability of being in state 1 - given by $p_n^*(s) = \Lambda^*(s)g_0^*$, where $\Lambda^*(s)$ is the Laplace transform of the distribution function of the event a forward takes place before a backward step takes place in the interval $(0, t)$. Of course, this is much harder to solve for because there are an infinite number of equations, and our naive attempts with a generating function have proved futile. However, we can solve it for the Poisson process as a "verification" (see Appendix).

Consider the question: what if the process does not ever hit site 1 with probability > 0? Such processes are known as terminating renewal process, (Karlin 1975 [20]). The mean number of renewals approach a finite value exponentially fast, meaning there is no mean velocity, and the process stops moving in a finite time.

However, if the time (a random variable T) until the next transition either forward or backward (whose density is $\lambda_i(t) + \mu_i(t)$) has finite mean, we can form another renewal process and we know that there will be an infinite number of renewals on average from Eq. (2.3). Now, consider $X(t)$ at the epochs when events occur. $X(t)$ at these epochs is a Markov chain (the imbedded chain). Then the problem can be cast in the form of a gambler's ruin problem [20], [15], and eventual probability of ever getting to state 1 depends solely on the probabilities p and q of going forward or backward. For us,

$$p = \int_0^\infty \lambda(t)\mathrm{d}t = \lim_{s \to 0} \lambda^*(s). \tag{4.13}$$

Since the time until the next transition is finite, it follows that $q = 1 - p$, and the probability of eventual absorption into state 1 given $X(0) = 0$ (and indeed any other initial state) is 1 if $p \geq q$. If $p < q$ we just define the first passage time to site -1 as the renewal increment, and obtain a negative velocity.

4.2.1 Extension to Spatially Periodic Forces

Suppose the external force $f(x)$ has a spatial periodicity that is an integer multiple N of the binding-site spacing L. Then, we can define the first passage time to site N as our renewal variable and proceed as described in the section above.

4.2.2 Computing Moments of the First Passage Time

While the construction of the renewal process using first-passage-time is fairly straightforward formally, what we are generally interested in are the mean and the variance, i.e., the moments. Computing this for non-exponential transition densities is hard, and so we resort to restricting the number of sites to a finite number, and increasing that number till the moments converge numerically to a value.

To elaborate, define a continuous time random walk on sites $\{1, 0, -1, -2, \cdots, -N\}$ with time-homogeneous transition densities λ and μ as before. Restrict k to $\{-1, \cdots, -N+1\}$ in Eq. (4.11) and make site $-N$ absorbing. Adding the equation,

32

$$g^*_{-N+1} = \mu g^*_{-N+2} \tag{4.14}$$

to the Eq. (4.11), we can again solve for the mgf of the first-passage-time and take the limit $s \to 0$ of the appropriate derivative numerically and get the moment we require, like in Eq. (2.17). Then, we make N larger until the required moment converges to within a numerical tolerance.

4.2.3 Randomness Parameter

It has been claimed in the literature (Svoboda 1993 [34]) that the inverse of the so-called randomness parameter r is a good measure of the number of "rate-limiting" steps in kinesin's enzymatic cycle. This is true for a Poisson process (Atzberger 2006 [2]) because if each "stepping" event consists of a sequence of n identical exponentially distributed elementary events, $1/r = n$. This, however, is not true if backward steps, or even there is a probability $p < 1$ that the motor steps forward or stays put. For example, in the PO model, this situation arises if $\beta_f = 0$.

We can apply renewal theory to get general expressions for r. Let each element in the renewal sequence X_k be made up of n identical exponentially distributed random variables with parameter λ. Let the reward sequence H_k take values ± 1 with probabilities p and q respectively with $p > q$. In terms of the cumulative reward $R(t)$, the randomness parameter can be defined as:

$$r = \lim_{t \to \infty} \frac{Var[R(t)]}{E[R(t)]} \tag{4.15}$$

From Eq. (2.35), one can write:

$$E[X_k] = \frac{n}{\lambda}, \tag{4.16}$$

$$Var[X_k] = \frac{n}{\lambda^2}, \tag{4.17}$$

$$E[H_k] = p - q, \tag{4.18}$$

$$Var[H_k] = p + q - (p - q)^2. \tag{4.19}$$

Then applying Eq. (2.49) for the variance of a reward process, we can write the randomness parameter as,

$$r = \frac{p - q}{n} + \frac{(p + q) - (p - q)^2}{p - q}. \tag{4.20}$$

Setting $q = 0$ in the above, we re-obtain $1/r = n$ for $p = 1$. Again, for $q = 0$, the inverse of the randomness parameter $1/r$ is plotted against the probability p for a few values of n in Fig. 4.1. Note that the randomness parameter serves its intended "purpose" only for $n = 1$ if there exists a possibility of backward steps. One can also show that if $p + q = 1$, the randomness parameter "prediction" for the number of steps in a process is off by a huge margin even when p is marginally less than 1. The discovery of processive backstepping in kinesin (Carter 2005 [7]) precludes the possibility that the randomness parameter will ever be useful in the study of kinesin.
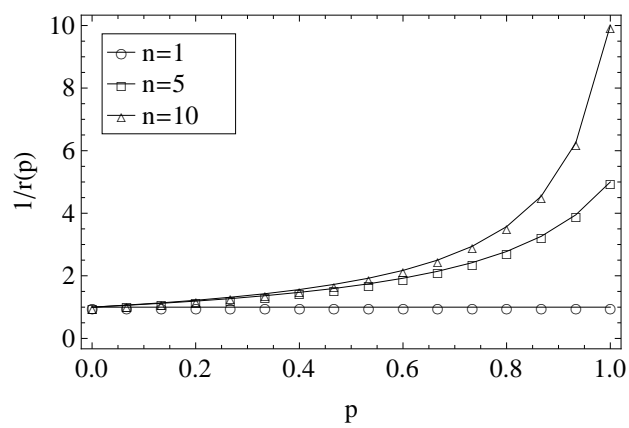
33

Figure 4.1: Variation of the randomness parameter with the probability of binding forward for different number of substeps in a Poisson-like process

Chapter 5

Multiple Motors

5.1 Modelling

Here, we use the basic PO model to characterize the motion of two kinesin motors pulling the bead cooperatively and make predictions regarding the cooperative behavior. The objective is to compare this with single-motor experiments, and to serve as a more severe test of the model.
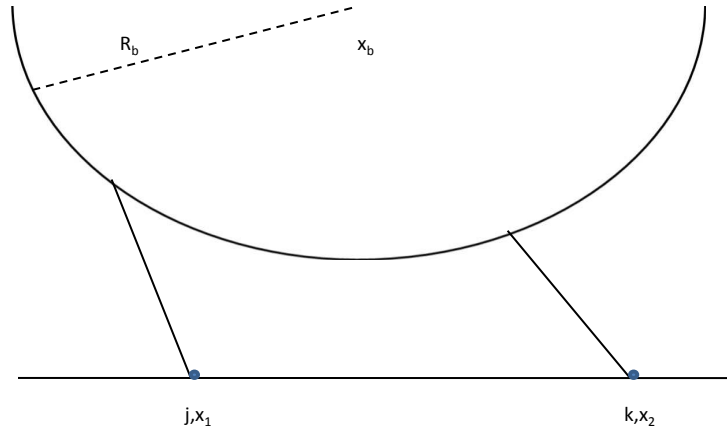

Figure 5.1: Schematic of likely typical experimental setup

The model requires very little modification. All we have to do is to keep track of an extra coordinate, that of the additional motor as shown schematically in Fig. 5.1. The state of the system is represented by $\{j, k\}$, where j and k can both be either integers or half-integers. If j (or k) is a half-integer, as before, it fixes the bound head location x_m, as in the single-motor PO model. If j or k is a half-integer, this means the head is unbound from the MT and is diffusing, and hence has another coordinate associated with it, the positions x_j and x_k respectively. The bead position is denoted x_b. There are three possible combinations of states - depending on whether the each motor has a head diffusing or not - and three associated potentials. The potential V is a function of the head locations (if applicable) x_j, x_k, bead position x_b and the separation between the motors $k-j$. The definitions of x_{bnd} and $x_{h_j(k)}$ are as before, and are uniquely determined by $x_{j(k)}$. One obtains,

$$V(x_j, x_k, x_b) = fx_b + \frac{K_{th}}{2}\left(x_{h_j} - x_{bnd}\right)^2 + \frac{K_{th}}{2}\left(x_{h_k} - x_b\right)^2 + W(x_j, x_k). \tag{5.1}$$

The biasing potential $W(x)$ depends on the state (j, k). Let $\mathbb{I}$ represent the set of integers, and let $\mathbb{H}$ be the set of half-integers. Then,

$$W(x_j, x_k) = \begin{cases} 0 & j \in \mathbb{I}, k \in \mathbb{I} \\ \frac{K_{bias}}{2}\left(x_{h_k} - (x_{bnd_j} + x_0)\right)^2 & j \in \mathbb{I}, k \in \mathbb{H} \\ \frac{K_{bias}}{2}\left(x_{h_j} - (x_{bnd_j} + x_0)\right)^2 + \frac{K_{bias}}{2}\left(x_{h_k} - (x_{bnd_j} + x_0)\right)^2 & j \in \mathbb{H}, k \in \mathbb{H} \end{cases} . \qquad (5.2)$$

We continue to make the assumptions made in the original PO model for a single motor plus a few more as follows

1. Each head equilibriates instantaneously with the bead when diffusing. This is still valid because of the ratio of diffusion coefficients $D_h/D_b \to \infty/$

2. The time scale of diffusion of the bead is still negligible. The tethers are in parallel, making the effective potential nearly twice as stiff, which makes the time-scale smaller than that for a single motor (see SecrefOU-process.

3. The head almost instantaneously binds to a binding site once hydrolysis completes. That is, the probability that the hydrolysis processes of both motors complete in the time required for binding is negligible.

It might turn out that when the motors are both perfectly synchronized, the hydrolysis processes might be coupled together possibly through some load dependence. Including the possibility that the hydrolysis processes complete together is not very hard. Here again, calculating the probabilities of binding forward and backward for each reduces to a first-passage problem in two variables. In our particular case, the problem is simple since the potentials that each head experiences are decoupled as $V(x_j, x_k, x_b) = V_1(x_j, x_b) + V_2(x_k, x_b)$, clearly, from Eq. (5.1). In general the equations are elliptic (but linear) and yield to simple finite-differencing schemes.

5.2   Simulation

As for a single motor, we construct a Markov chain, with the states and transitions as defined in Fig. 5.2. The only complication here is that the state-space is infinite, and the entries of the Markov chain depend on the state. We have to calculate each entry numerically, and there are limited analytical options - no renewal theory to the rescue here.

To circumvent this problem, we resort to a truncation. We choose a sufficiently large number of binding sites $(-N, N)$, and make the boundaries absorbing, by stating that once either motor reaches $\pm N$, they get absorbed and cannot move. We then simulate the governing differential equations for the probabilities of being in each site, given different initial configurations.

Let $C_{j,k}$ be the probability of being in state $\{j, k\}$. Let $P_{j,k}$ represent the probability of binding forwards for a motor - whether it is for the motor at j or k depends on whether they are integers or half-integers. When the motors are both diffusing - j and k are both half-integers - and hydrolysis completes, either motor binds instantaneously and we must calculate two probabilities of binding forwards for each motor $P1_{j,k}$, $P2_{j,k}$ associated with state $\{j, k\}$. The other chemical parameters are α, β and γ, the same as the PO model. We need to write four different types of differential equations for the four different kinds of states. Then, for $-N + 1 < j, k < N - 1$ one obtains,
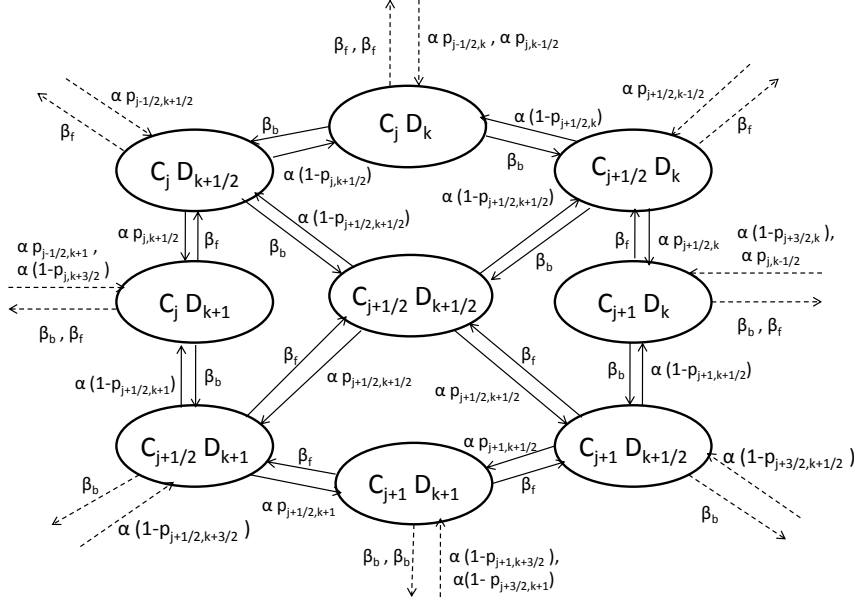
Figure 5.2: Possible State Transitions

$$\frac{\mathrm{d}C_{j,k}}{\mathrm{d}t} = \begin{cases} \begin{aligned} &\alpha P_{j-1/2,k}C_{j-1/2,k} + \alpha P_{j,k-1/2}C_{j,k-1/2}+ \\ &\alpha(1 - P_{j+1/2,k})C_{j+1/2,k} + \alpha(1 - P_{j,k+1/2})C_{j,k+1/2}+ \\ &-2(\beta_b + \beta_f)C_{j,k} \end{aligned} & j \in \mathbb{I}, k \in \mathbb{I} \\[2em] \begin{aligned} &\alpha P_{j-1/2,k}C_{j-1/2,k} + \alpha(1 - P_{j+1/2,k})C_{j+1/2,k}+ \\ &\beta_b C_{j,k-1/2} + \beta_f C_{j,k+1/2}+ \\ &(\beta_b + \beta_f + \alpha)C_{j,k} \end{aligned} & j \in \mathbb{I}, k \in \mathbb{H} \\[2em] \begin{aligned} &\beta_b C_{j-1/2,k} + \beta_f C_{j+1/2,k}+ \\ &\beta_b C_{j,k-1/2} + \beta_f C_{j,k+1/2} - 2\alpha C_{j,k} \end{aligned} & j \in \mathbb{H}, k \in \mathbb{H} \end{cases} \tag{5.3}$$

In Eq. (5.3), note that for each differential equation, there are source terms from the neighbouring states from which the system can enter that particular state and one decay term for the rate at which the system leaves that particular state. So, for the boundary equations - if $|j|, |k| > N - 1$ in Eq. (5.3) - drop appropriate decay term and source terms if $j, k = \pm N$.

The next step is to calculate the total probabilities for each relevant state. The procedure is essentially that described in Section 3.2 for a single motor. If there is only one diffusing head (and suppose it is k) determine the head density $\rho(x_k|x_b)$ and determine the conditional probability of binding forward $\pi(x_k, x_b)$, using equations exactly like Eq. (3.11). The total probability $P_{j,k}(f)$ follows immediately.

If both motors are diffusing, the conditional densities and probabilities continue to be *independent*, $\rho(x_j|x_b)$, $\rho(x_k|x_b)$, $p_t(x_j, x_b)$ and $p_t(x_k, x_b)$ because of the way the potential decouples as mentioned in Section 5.1 and the total probabilities of binding forwards can be written in terms of the the effective potential ($V_{eff}(x_b)$) and bead density ($\rho_{bead}(x_b)$) as,

$$V_{eff}(x_b) = -k_B T \log \left(\int_{-(k-3/2)L}^{(k+1/2)L} \exp \frac{-V_1(x_k, x_b)}{k_B T} \mathrm{d}x_k \int_{-(j-3/2)L}^{(j+1/2)L} \exp \frac{-V_2(x_j, x_b)}{k_B T} \mathrm{d}x_j \right), \quad (5.4)$$

$$P1_{j,k}(f) = \int_{-\infty}^{\infty} p_t(x_j, x_b) \rho_{bead}(x_b) \mathrm{d}x_b, \quad (5.5)$$

$$P2_{j,k}(f) = \int_{-\infty}^{\infty} p_t(x_k, x_b) \rho_{bead}(x_b) \mathrm{d}x_b. \quad (5.6)$$

There are a few homogeneities in the problem we can exploit to ease computational effort: any state (j, k) is identical to $\{0, k - j\}$ (or $\{1/2, k - j\}$ if j is a half-integer) but for an origin shift of jL. Since the motors are identical, parameters like the probability of binding forward, potential energy, are independent of the identity of the motor. When the motors are both diffusing, again because of the obvious homogeneity, if state $\{j, k\}$ has probabilities $P1_{j,k}, P2_{j,k}$, state $\{j_1, k_1\}$ with $j_1 = k, k_1 = j$, has probabilities $P2_{j,k}, P1_{j,k}$. These observations significantly reduce the number of calculations.

5.3 Results

The two motors were simulated on a grid with $(-50, 50)$ binding sites at two ATP concentrations - the same as the single-molecule data - for a range of forces $(-4.5, 9.5)$ pN. The ODEs in Eq. (5.3) were simulated for a time such that edge-effects, i.e., the effect of the absorbing binding sites at $(-50, 50)$ on the motor dynamics was negligible. Data was obtained for different initial configurations.

The multiple motor data is plotted against the single-motor predictions for the two different ATP concentrations in Fig. 5.3. Notice that at strongly assisting loads, the mean velocity of the bead is lower than the single-motor, owing to the fact that at least two ATP hydrolyses need to occur to move 8 nm. However, because the load is shared between the two motors, the stall force is extended to nearly twice the stall-force of a single motor. We will explore different aspects of the motor and bead dynamics in the following sections.

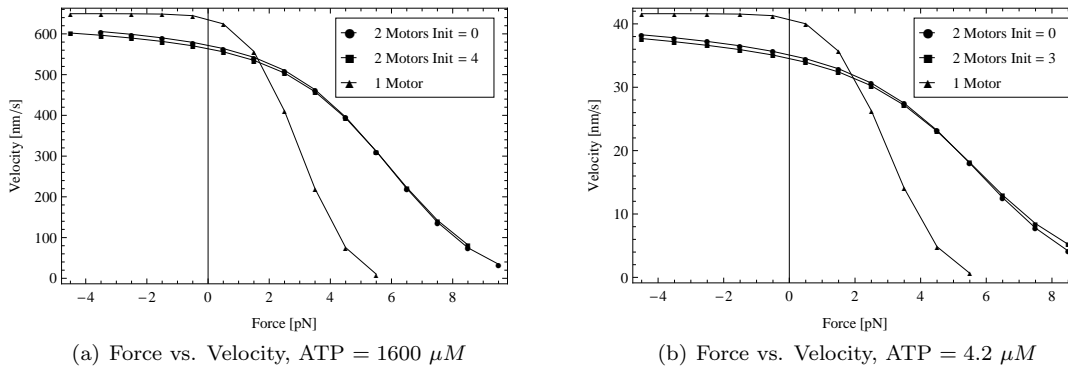(a) Force vs. Velocity, ATP = 1600 μM (b) Force vs. Velocity, ATP = 4.2 μM

Figure 5.3: Two motors pulling a bead: force velocity data for different ATP concentrations compared with single motor predictions using the PO model. The multiple motor data is obtained for different initial motor configurations, and since the motors synchronize, the velocity predictions are nearly identical.

5.3.1 Motor Dynamics

A general conclusion from the detailed numerical study performed is that the motor synchronize for all different initial spatial separations for high and low ATP concentrations. The reason lies in the proba-

bility of binding forwards depending on the relative states of the motors $\{j, k\}$. As mentioned before, the probability depends only on the relative separation $(j - k)$; moreover, there are two probabilities when j and k are both half-integers. The probabilities are plotted in Fig. 5.4(a) for a low and high force - clearly these are dependent solely on mechanical parameters - with $j = 0$ in Fig. 5.4(a) and $j = 1/2$ in Fig. 5.4(b). It is clearly seen that the lagging motor has a much larger tendency to bind forwards in both cases: when the leading motor is bound firmly to the MT, and when it has bound ATP and one of its heads is diffusing.
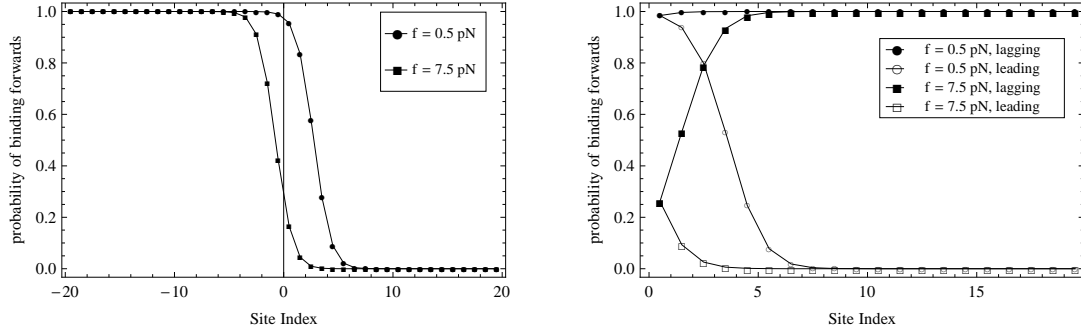
(a) Probability of binding forwards vs. site index k. $j = 0$ fixed.

(b) The two probabilities of binding forwards when both diffusing vs. site index k. $j = 1/2$ fixed.

Figure 5.4: Probabilities of motors binding to the forward site, and its dependence on the relative states - spatial separation and phase - of the two motors
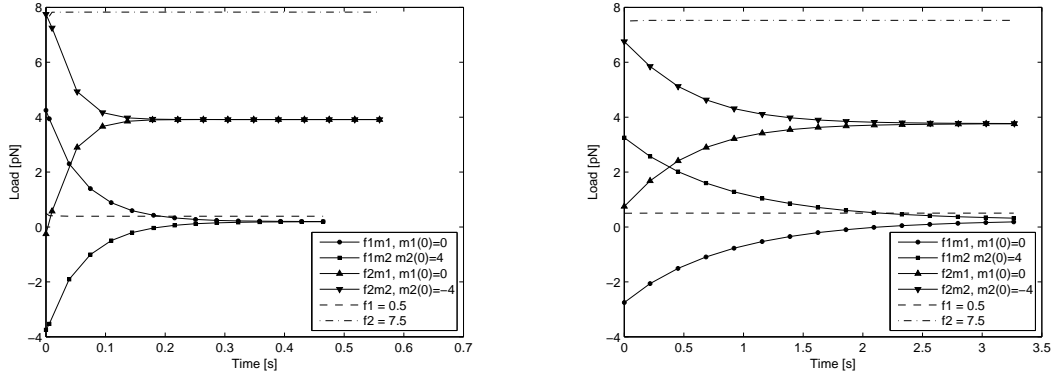

(a) Load on each motor vs. time. motor1$(t = 0) = 0$, motor2$(t = 0) = 4, -4$, ATP $= 1600 \ \mu M$

(b) Load on each motor vs. time. motor1$(t = 0) = 0$, motor2$(t = 0) = 4, -4$, ATP $= 4.2 \ \mu M$

Figure 5.5: Load sharing between the two motors for high and low ATP and load. The $- - -$ line shows the sum of the individual loads. It is a constant, as expected.

A more physical picture is seen in Fig. 5.5. Here, the mean load "felt" by each motor - i.e., the extention of its tether - is plotted as a function of time. Figure 5.5 shows that while the total load, as it must be, is constant and equal to the external force, the load on each individual motor varies until it is shared equally on the two motors. Hence, it is unsurprising that the expected positions of the motor locations synchronize. A plot of the individual motor positions(Fig. 5.6) shows a dynamic picture of the motor synchronization process. We obtained plots for low and high ATP concentrations and loads to indicate that this synchronization happens for the whole parameter range we considered. Note that at low ATP, it takes a longer time for the load to be equally shared and for the motors to synchronize

- this is a consequence of the lower rate of stepping. But at higher loads, synchronization happens faster than at lower loads. The reason this happens is indicated by the probabilities of binding forward in Fig. 5.4(a), which shows that the probability of binding forward for the leading motor falls to zero quicker at higher loads than at lower loads. Another observation is that the leading motor "waits" for the lagging motor to catch up. Again, this fact is easily reconciled with the data from Fig. 5.4.
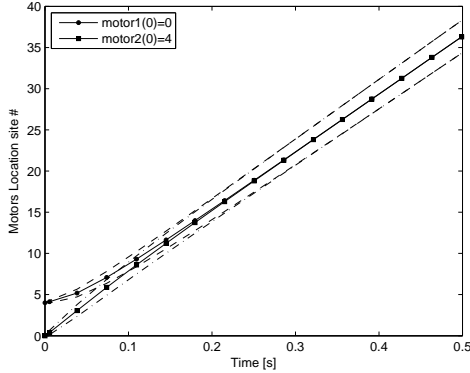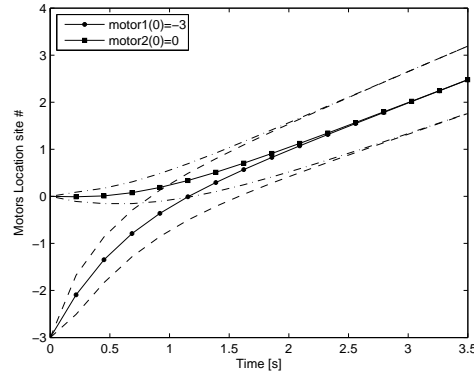

(a) Motor position (site index) vs. time for both motors, different initial separation. $f = 0.5$, ATP $= 1600 \ \mu M$
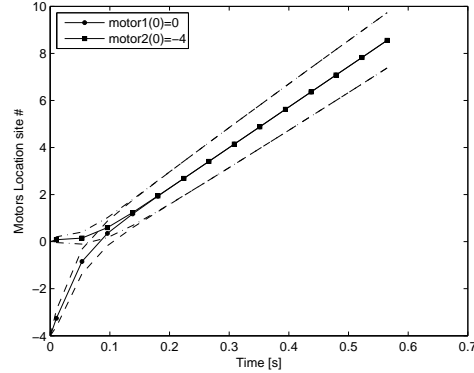
(b) Motor position (site index) vs. time for both motors, different initial separation. $f = 7.5$, ATP $= 1600 \ \mu M$
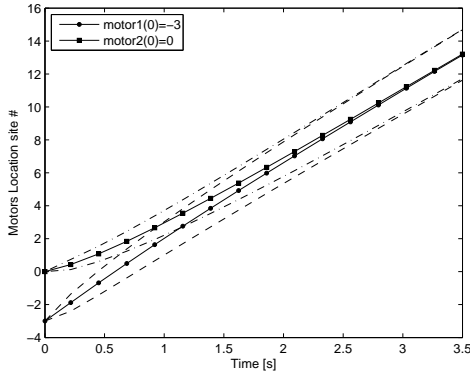
(c) Motor position (site index) vs. time for both motors, different initial separation. $f = 0.5$, ATP $= 4.2 \ \mu M$

(d) Motor position (site index) vs. time for both motors, different initial separation. $f = 7.5$, ATP $= 4.2 \ \mu M$

Figure 5.6: Motor position vs. time for different initial separations, loads and ATP. Note how the motors synchronize under all conditions

5.3.2 Bead Variance and Randomness

The bead position and it's standard deviation is easily obtained from the relative motor positions. To calculate the randomness parameter, let $x_b(t)$ be the bead position so that,

$$r = \lim_{t \to \infty} \frac{Var[x_b(t)]}{E[x_b(t)]L} = \lim_{t \to \infty} \frac{Var[x_b(t)]}{t} \frac{t}{E[x_b(t)]} \frac{1}{L}. \tag{5.7}$$

The most direct way to calculate the randomness parameter is to solve Eq. (5.3) for a long time interval, and find the variance and expected value and take their ratio. However, it is noticed in Fig. 5.7(a) that the randomness parameter has not quite reached it's steady-state value. However, it is reasonable to believe that if computed for a larger time interval, it will indeed reach a limiting value. We know

from renewal theory for a single motor, that the rations $E[x_b(t)]/t$ and $Var[x_b(t)]/t$ approach constant limits as $t \to \infty$. Since, essentially, this is also a renewal process - but with a much more complicated reward function - a similar limit is to be expected. Hence, a better estimate of the randomness paratemer would be to compute the slopes of the mean and variance of $x_b(t)$ for a large time t. This is shown in Fig. 5.7(b).

(a) Randomness Parameter vs. t, ATP $= 1600 \ \mu M$

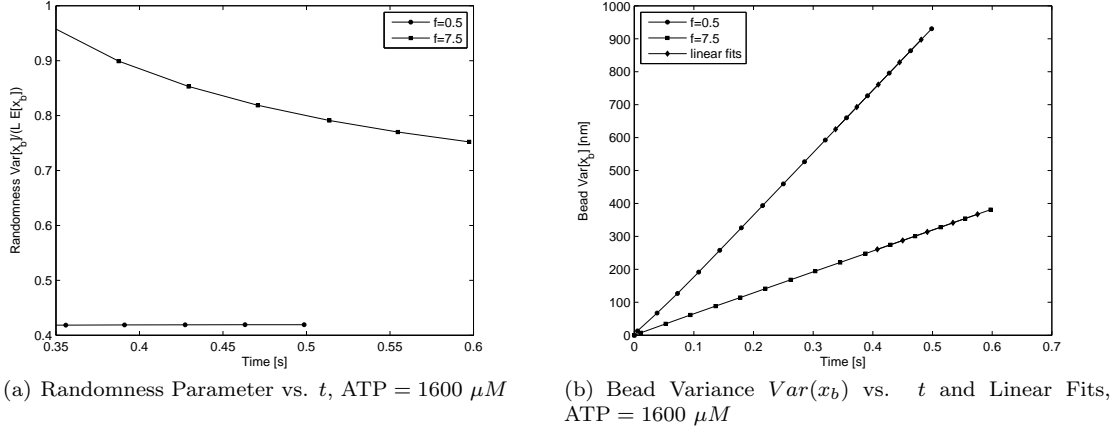(b) Bead Variance $Var(x_b)$ vs. t and Linear Fits, ATP $= 1600 \ \mu M$

Figure 5.7: Evolution of the bead variance and randomness parameter with time for the higher ATP concentration

The randomness parameter computed by the two methods is shown in Fig. 5.8 and is compared with the single motor predictions. It is noticed that the randomness parameter is lower for all forces. A not-very-convincing way to physically justify is this is to for each renewal - one motor completes a step - the bead steps only by $L/2$, and one might argue based on the general properties of the randomness parameter for Poisson processes that now both motors have to complete a step for the bead to move $8 \ nm$.
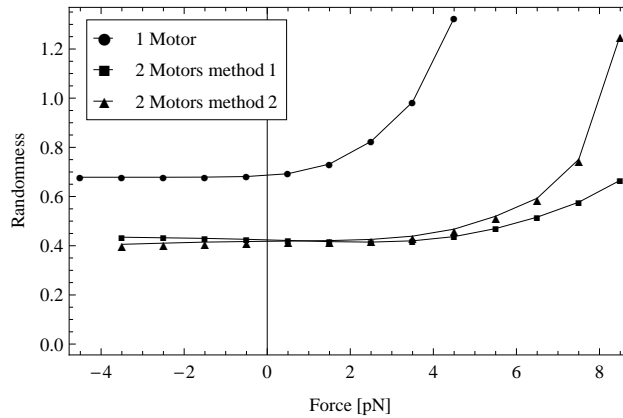

Figure 5.8: Force vs. Randomness for two motors computed by two different methods and one motor from the PO model

41

Chapter 6

Summary and Future Work

A short summary of the work done in this study are:

1. Mathematical justification of the various assumptions in the PO model, and some commentry on it's deficiencies.

2. Application of Renewal Theory to modeling kinesin and derivation of some known results as a verification.

3. Different methods based on Renewal Theory to extend the pO model to incorporate more realistic modelling of the chemistry, diffusion and variable forces.

4. Application of the PO model to multiple motors - specifically two - and a discussion of the various predictions that it makes.

The potential for future work includes:

1. Application of the different methods outlined to make actual predictions for variable forces, non-Markovian chemistry etc.

2. More complicated models for the different structural elements in kinesin starting with, say, a more realistic potential energy.

3. Extending renewal theory to handle multiple minima in the potential to predict other aspects such as detachment rates of kinesin. (Mogilner 2001 [23]).

Appendix A

Renewal Theory for a Poisson Random Walk

This Appendix is included merely because it contains a few useful techniques using probability generating functions, and to illustrate the technique described in Section 4.2. Let $X(t)$ be a stochastic process giving the position of a Poisson stepper at time t. It steps up or down by integer increments when a forward or backward stepping event take place. Let $p_i(t)$ be the probability that $X(t) = i$ given $X(0) = 0$. Now, what we wish to find is the "velocity" $(v(t))$ of the process $dE[X(t)]/dt$. Define a probability generating function $G(z,t) = \Sigma_i = -\infty^{infty} z^i p_i(t)$ and notice that the first moment is $M_1 = E[X(t)] = \lim_{z \to 1} \partial G / \partial z$. Clearly, we are looking for $v(t) = dM_1/dt$. Then one may write:

$$\frac{dp_i(t)}{dt} = \lambda p_{i-1} + \mu p_{i+1} - (\lambda + \mu) p_i \tag{A.1}$$

Multiplying by z^i summing the above

$$\frac{\partial G(z,t)}{\partial t} = z\lambda G + \frac{\mu G}{z} - (\lambda + \mu)G \tag{A.2}$$

We can solve this equation easily with the obvious boundary conditions $G(z,0) = 1$ and $G(1,t) = 1$ - since this is standard procedure, we will dispense with details. Then, we find that the velocity is given by:

$$v(t) = \lambda - \mu \quad \lambda > \mu > 0 \tag{A.3}$$

We will now calculate the velocity using the first passage time, and the formulas of renewal theory from Section 2.3, using a technique from the theory of immigration-emigration processes.

Let T now be the first passage time to site 1 with density $f(t)$ and distribution $F(t)$. Setup an absorbing barrier at site $X = 1$ and write the Laplace transform of $f(t)$ as:

$$Prob\{T < t\} = F(t) = p_i(t), \tag{A.4}$$

$$E[e^{-sT}] = \int_0^\infty e^{-st} \frac{dF(t)}{dt} = s p_i^*(s) - p_i(0). \tag{A.5}$$

Next we Laplace transform Eq. A.1 and make the necessary modifications to it to account for the absorbing barrier as follows:

$$\frac{dp_1(t)}{dt} = \lambda p_0, \tag{A.6}$$

$$\frac{dp_0(t)}{dt} = \lambda p_1 - (\lambda + \mu)p_0, \tag{A.7}$$

$$\frac{dp_i(t)}{dt} = \lambda p_{i-1} + \mu p_{i+1} - (\lambda + \mu)p_i. \tag{A.8}$$

Then redefine the generating function $G(z,t) = \Sigma^1_{-\infty} z^{-i} p_i(t)$ (which looks like a Laurent series). The boundary conditions are the same as above, and we can write an equation in terms of the Laplace transform of the generating function.

$$G^* = \frac{p_1^*}{z} + p_0^* + z p_{-1}^* + \cdots, \tag{A.9}$$

$$G^* = \frac{p_1^*(z^2\mu - (s+\lambda+\mu)z + \lambda) + p_1^* s z + z^2}{(z^2\mu - (s+\lambda+\mu)z + \lambda)}. \tag{A.10}$$

The above expression for $G^*(s,z)$ must be analytic for in $0 < z \le 1$ since $\Sigma^1_{i=-\infty} p_i(t) = 1$. But we can show that the denominator has one root $z_0(s)$ that is always in $(0,1]$ for all $Re(s) > 0$. Thus, the numerator must also have a root at $z_0(s)$. This yields an expression for $p_1^*(s)$, and we can differentiate it to extract the first moment of T. It turns out, after a little bookwork, that:

$$p_1^*(s) = \frac{(s+\lambda+\mu) - \sqrt{(s+\lambda+\mu)^2 - 4\lambda\mu}}{2s\mu}, \qquad \forall \lambda > \mu > 0, \tag{A.11}$$

$$E[T] = -\lim_{s \to 0} \frac{d}{ds}(s p_1^*(s)) = \frac{1}{\lambda - \mu}. \tag{A.12}$$

44

Bibliography

[1] R.D. Astumian and P. Haenggi. Brownian motors. *Physics Today*, 55(11):33–39, 2002.

[2] P.J. Atzberger and C.S. Peskin. A Brownian Dynamics Model of Kinesin in Three Dimensions Incorporating the Force-Extension Profile of the Coiled-Coil Cargo Tether. *Bulletin of Mathematical Biology*, 68(1):131–160, 2006.

[3] M. Badoual, F. Jülicher, and J. Prost. Bidirectional cooperative motion of molecular motors. *Proceedings of the National Academy of Sciences of the United States of America*, 99(10):6696, 2002.

[4] M. Bier. Brownian ratchets in physics and biology. *Contemporary Physics*, 38(6):371–379, 1997.

[5] S.M. Block. Probing the kinesin reaction cycle with a 2 D optical force clamp. *Proceedings of the National Academy of Sciences*, 100(5):2351–2356, 2003.

[6] S.M. Block. Kinesin Motor Mechanics: Binding, Stepping, Tracking, Gating, and Limping. *Biophysical Journal*, 92(9):2986, 2007.

[7] N.J. Carter and R.A. Cross. Mechanics of the kinesin step. *Nature*, 435(7040):308–312, 2005.

[8] E. Cinlar. Introduction to Stochastic Processes. *Englewood Cliffs*, 1975.

[9] D.R. Cox and H.D. Miller. *The Theory of Stochastic Processes*. Chapman & Hall/CRC, 1977.

[10] R.A. Cross. The kinetic mechanism of kinesin. *Trends in Biochemical Sciences*, 29(6):301–309, 2004.

[11] I. Derenyi and T. Vicsek. The Kinesin Walk: A Dynamic Model with Elastically Coupled Heads. *Proceedings of the National Academy of Sciences of the United States of America*, 93(13):6775–6779, 1996.

[12] R.H. Dillon and L.J. Fauci. An Integrative Model of Internal Axoneme Mechanics and External Fluid Dynamics in Ciliary Beating. *Journal of Theoretical Biology*, 207(3):415–430, 2000.

[13] M.E. Fisher and A.B. Kolomeisky. Simple mechanochemistry describes the dynamics of kinesin molecules. *Proceedings of the National Academy of Sciences*, page 141080498, 2001.

[14] S.P. Gilbert, M.R. Webb, M. Brune, and K.A. Johnson. Pathway of processive ATP hydrolysis by kinesin. *Nature*, 373(6516):671, 1995.

[15] G. Grimmett and D. Stirzaker. *Probability and Random Processes*. Oxford University Press, USA, 2001.

[16] N.R. Guydosh and S.M. Block. Backsteps induced by nucleotide analogs suggest the front head of kinesin is gated by strain. *Proceedings of the National Academy of Sciences*, 103(21):8054–8059, 2006.

[17] AG Hendricks, BI Epureanu, and E. Meyhofer. IMECE2006-15752 Synchronization of Motor Proteins Coupled Through a Shared Load. *ASME Applied Mechanics Division-Publications-AMD*, 257:489, 2006.

[18] J.P. Hespanha. A model for stochastic hybrid systems with application to communication networks. *Nonlinear Analysis*, 62(8):1353–1383, 2005.

[19] J. Hu, J. Lygeros, and S. Sastry. Towards a theory of stochastic hybrid systems. *Hybrid Systems: Computation and Control*, 1790:160–173, 2000.

[20] S. Karlin and H.M. Taylor. *A First Course in Stochastic Processes*. Academic Press, 1975.

[21] H.M. Lacker and C.S. Peskin. Control of Ovulation Number in a Model of Ovarian Follicular Maturation. *Some Mathematical Questions in Biology*, 14, 1981.

[22] R.E. Mirollo and S.H. Strogatz. Synchronization of pulse-coupled biological oscillators. *SIAM Journal of Applied Mathematics*, 50(6):1645–1662, 1990.

[23] A. Mogilner, A.J. Fisher, and R.J. Baskin. Structural Changes in the Neck Linker of Kinesin Explain the Load Dependence of the Motor's Mechanical Cycle. *Journal of Theoretical Biology*, 211(2):143–157, 2001.

[24] F.J. Nedelec, T. Surrey, A.C. Maggs, and S. Leibler. Self-organization of microtubules and motors. *Nature*, 389(6648):305–8, 1997.

[25] C.S. Peskin and G. Oster. Coordinated hydrolysis explains the mechanical behavior of kinesin. *Biophysical Journal*, 68(4 Suppl), 1995.

[26] E.M. Purcell. Life at low Reynolds number. *American Journal of Physics*, 45(1):3–11, 1977.

[27] H. Qian and E. L. Elson. Single-molecule enzymology: stochastic Michaelis–Menten kinetics. *Biophysical Chemistry*, 101:565–576, 2002.

[28] P. Reimann and P. Hänggi. Introduction to the physics of Brownian motors. *Applied Physics A: Materials Science & Processing*, 75(2):169–178, 2002.

[29] S. Rice, A.W. Lin, D. Safer, C.L. Hart, N. Naber, B.O. Carragher, S.M. Cain, E. Pechatnikova, E.M. Wilson-Kubalek, M. Whittaker, et al. A structural change in the kinesin motor protein that drives motility. *Nature*, 402:778–784, 1999.

[30] S.S. Rosenfeld, P.M. Fordyce, G.M. Jefferson, P.H. King, and S.M. Block. Stepping and Stretching: How Kinesin Uses Internal Strain to Walk Processively. *Journal of Biological Chemistry*, 278(20):18550–18556, 2003.

[31] S.M. Ross. *Stochastic Processes [M]*. John Willey &Sons, 1983.

[32] A.J.F. Siegert. On the First Passage Time Probability Problem. *Physical Review*, 81(4):617–623, 1951.

[33] S.H. Strogatz. From Kuramoto to Crawford: exploring the onset of synchronization in populations of coupled oscillators. *Physica D: Nonlinear Phenomena*, 143(1-4):1–20, 2000.

[34] K. Svoboda, C.F. Schmidt, B.J. Schnapp, and S.M. Block. Direct observation of kinesin stepping by optical trapping interferometry. *Nature*, 365(6448):721–727, 1993.

[35] S. Uemura, K. Kawaguchi, J. Yajima, M. Edamatsu, Y.Y. Toyoshima, and S. Ishiwata. Kinesin-microtubule binding depends on both nucleotide state and loading direction. *Proceedings of the National Academy of Sciences*, 99(9):5977, 2002.

[36] G.E. Uhlenbeck and L.S. Ornstein. On the Theory of the Brownian Motion. *Physical Review*, 36(5):823–841, 1930.

[37] R.D. Vale, T. Funatsu, D.W. Pierce, L. Romberg, Y. Harada, and T. Yanagida. Direct observation of single kinesin molecules moving along microtubules. *Nature*, 380(6573):451–453, 1996.

[38] A.T. Winfree. Biological rhythms and the behavior of populations of coupled oscillators. *J Theor Biol*, 16(1):15–42, 1967.

[39] A. Yildiz, M. Tomishige, R.D. Vale, and P.R. Selvin. Kinesin Walks Hand-Over-Hand. *Science*, 303(5658):676–678, 2004.